Arab J Sci Eng (2013) 38:221–249
DOI 10.1007/s13369-012-0450-8

REVIEW ARTICLE - SPECIAL ISSUE - MECHANICAL ENGINEERING

Thermodynamic Analysis

Yaşar Demirel

Received: 28 March 2012 / Accepted: 19 April 2012 / Published online: 9 January 2013

Abstract This review mainly summarizes some of the developments on the various aspects of thermodynamic analysis within the past 15 years. Therefore, it is limited and will omit some valuable work unintentionally, mainly because of the vast number of publications in the field. The thermodynamic analyses mainly aim at assessing the thermodynamic imperfections and suggest possible ways of improving these imperfections. In this review, thermodynamic analyses have been summarized under these methodologies: (i) second law analysis, (ii) exergy analysis, (iii) pinch analysis, (iv) equipartition principle, (v) Gibbs free energy minimization, (vi) thermoeconomics, (vii) exergoeconomics, and (viii) extended exergy analysis. The exergy analysis, which is the most popular methodology, is discussed for the following systems: (1) power cycle applications, (2) biomass and coal gasification, (3) solar energy applications, (4) refrigeration, (5) waste heat utilization, (6) distillation column systems, and (7) heat and fluid flow in micro channels. Besides that, statistical and non equilibrium thermodynamics are discussed briefly. One of the main conclusions of this review is that thermodynamic analysis has been confined mainly to heat and fluid flow systems. Thermodynamic analysis with its unifying power may be more useful and effective if it is successfully expanded toward diverse and multi-scale processes in physical, chemical, and biological systems.

Keywords Second law analysis · Exergy analysis · Pinch analysis · Equipartition principle · Gibbs free energy minimization · Thermoeconomics · Extended exergy analysis

Y. Demirel (✉)
Department of Chemical and Biomolecular Engineering, University of Nebraska Lincoln, Lincoln, NE 68588, USA
e-mail: ydemirel2@unl.edu

الخلاصة

تلخص هذه المراجعة الأدبية أساس بعض التطورات في تحليل الديناميكا الحرارية خلال الخمس عشرة سنة الأخيرة. لذلك هي محدودة ، وسوف تهمل بعض الأعمال القيمة من دون سوء نية، وذلك أساسٌ للعدد الهائل من النشرات العلمية في تحليل الديناميكا الحرارية لأنظمة متعددة. وتهدف تحاليل الديناميكا الحرارية غالبا إلى تقييم تشوهات الديناميكا الحرارية ، وتقترح طرقا متعددة لتحسين هذه التشوهات. وفي هذه المراجعة الأدبية تم تلخيص تحاليل الديناميكا الحرارية تحت هذه المنهجيات: (أ) تحليل القانون الثاني (ب) تحليل إكزيرجي (ج) تحليل الرف (د) مبدا التقسيم المتساوي (هـ) تقليل طاقة جيبس الحرة (و) الاقتصادية الحرارية (ز) اقتصادية إكزيرجي (ح) تحليل إكزيرجي الممتد. وتمت مناقشة تحليل إكزيرجي، وهي المنهجية الأكثر شهرة، للأنظمة التالية: (1) تطبيقات دورة الطاقة (2) تحويل الفحم والكتلة الحيوية إلى غاز (3) تطبيقات الطاقة الشمسية (4) التبريد (5) الاستفادة من حرارة الفضلات (6) أنظمة التقطير بالعمود. وأحد أهم الاستنتاجات لهذه المراجعة الأدبية هو أن تحليل الديناميكا الحرارية يقتصر غالبا على أنظمة الحرارة وتدفق السائل. إن تحليل الديناميكا الحرارية مع مداه العريض قد يكون مفيدا وفعالا إذا تم توسيعه بنجاح باتجاه عمليات متنوعة ومتعددة المقاييس في الأنظمة الفيزيائية والكيميائية والحيوية.

List of Symbols

a_1, a_2	Parameters in Eq. (6.9)
A	Affinity, J mol^{-1}; availability, kJ kg^{-1}
$\breve{A}$	Affinity, J mol^{-1}
Be	Bejan number
c_p	Heat capacity, J kg^{-1} K^{-1}
C_i	Concentration of specie i, mole m^{-3}
$\mathrm{d_e}$	Exchange through the boundary
$\mathrm{d_i}$	Internal change
Da	Damköhler number, dimensionless
D_i	Diffusion coefficient of species i, m^2 s^{-1}
$D_{S,e}$	Effective diffusion coefficient for the substrate S, m^2 s^{-1}
$D_{D,e}$	Coupling coefficient related to the Dufour effect, J m^2 mol^{-1} s^{-1}

$D_{T,e}$ Coupling coefficient related to the thermal diffusion (Soret effect), mol m^{-1} s^{-1} K^{-1}
e Energy source per unit volume (W/m^3),
ex Specific exergy, kW kg^{-1}
ex_f Exergy flow, kW kg^{-1}
Ex Exergy, kW
E Activation energy of the chemical reaction, J mol^{-1}
F Faraday constant
H Enthalpy, kJ/kg
ΔH_r Reaction enthalpy, J mol^{-1}
I Current, A
g Gravitation acceleration, m s^{-2}
G Gibbs free energy
J Diffusive mass flux (flow), mol m^{-2} s^{-1}
J_q Conduction heat flux (flow), W m^{-2}
J_r Volumetric reaction rate, mol m^{-3} s^{-1}
K Thermal conductivity
k_e Effective thermal conductivity, W m^{-1} K^{-1}
k_B Boltzmann constant
k_i Rate constant for chemical reaction i
K Equilibrium constant
L_{ik} Phenomenological coefficients
L_{qr} Element of coupling coefficient between chemical reaction and heat flow, mol K/(m^2 s)
L_{ir} Element of coupling coefficient between chemical reaction and mass flow, mol^2 K/(J m^2 s)
Le Modified Lewis number, dimensionless
L_{ik} Phenomenological coefficients
L_{qr} Coupling coefficient between chemical reaction and heatflow, mol K m^{-2} s^{-1}
L_{Sr} Coupling coefficient between chemical reaction and massflow, mol^2 K J^{-1} m^{-2} s^{-1}
m Mass, kg
n Number of moles, number of components
N Amount, mole, kg
N_r Number of independent reactions
Q Partition function
p_i Probability
P Pressure, kPa; total entropy production, kJ K^{-1}
$P*$ Saturation pressure
q Conduction heat flow, W/m^2
q_C Condenser duty, W
q_R Reboiler duty, W
$\mathbf{r}$ Spacial vector, m
R Gas constant, kJ mol^{-1} K^{-1}
S Entropy, kJ K^{-1}
$\dot{S}_{prod}$ Rate of entropy production
t Time, s^{-1}
T Temperature, K
T_o Reference temperature
u Internal energy
v Velocity m s^{-1}
V Total volume, m^3
y gas phase composition
W Work
x Thermodynamic force ratio
X Thermodynamic force
z Elevation, dimensionless distance; charge
Z Phenomenological stoichiometry; partition function, configuration integral

Greek Letters

α Number of atoms
γ Arrhenius group, dimensionless
ε Cross coefficient related to Soret effect,dimensionless
η Energy conversion efficiency
θ Dimensionless concentration defined
κ Cross coefficient dimensionless
μ Chemical potential, J/mol
ρ Density, kg/m^3
σ Entropy production; cross coefficient, dimensionless
τ Dimensionless time
τ_q Phase-lag in the heat flux
τ_T Phase-lag in the temperature gradient
Θ Viscous dissipation function, s^{-2}
φ Dimensionless temperature
ω Cross coefficient related to Dufour effect, dimensionless
θ Dimensionless composition
λ Relation in Eq. (7.1)
ν Stoichiometric coefficient
ψ Electric potential, V
τ Dimensionless time
ω Dimensionless parameter related to Dufour effect

Subscripts

b Backward
D Dufour
e Effective
ext External
eq Equilibrium
f Forward
r Reaction
S Soret

1 Introduction

Energy has several forms, each endowed with a different quality. The quality of an energy flux is a measure of its capacity to cause change. We can identify 'ordered' or 'high-quality' energy forms (potential, kinetic, mechanical, electrical) that can be ideally converted into each other with 100 % efficiency. There are other forms of energy, such as internal, kinetic, chemical, and thermal that cannot be converted into each other without an intrinsic efficiency loss. Since energy

is conserved, the difference $E_{\text{in}} - E_{\text{out}}$ must be accounted for 'dissipated' energy into a low-temperature flux absorbed or provided by the environment. The 'environment' is a system so large that its properties (pressure, temperature, chemical composition, kinetic or potential energy, etc.) are not affected by the interaction with the man-made system. These considerations, although formally incomplete from a scientific point of view, convey the correct information in an easily understandable form.

The French physicist G. Gouy in 1889 and the Swiss engineer A Stodola in 1905 independently stated that the lost available work is directly proportional to the rate of entropy production due to irreversibility in non equilibrium systems with exchange of energy and momentum within the fluid and at the boundaries. This statement was made more explicit, at least, for the thermal systems that the irreversibility is directly proportional to the rate of entropy production. So the rate of entropy production became crucial parameter in the art of thermal systems. The design questions that followed the Gouy–Stodola theorem are

- What is the total rate of entropy production?
- How the entropy production is distributed through the system?
- How to design a thermal system to produce the least possible entropy production?

This review consists of thermodynamic analyses related to improving the thermodynamic imperfections in various systems [1–25]. Thermodynamic analyses include second law analysis, exergy analysis, pinch analysis, equipartition principle, Gibbs free energy minimization, thermoeconomics, exergoeconomics, and extended exergy analysis. All of these analyses and their applications are very much an exertion of thermodynamics improvements into the design and simulation of thermal engineering systems. Some of the systems are more energy intensive than others. The more traditional use of the exergy analysis is for heat engines to produce power and electricity, combined heat and power schemes, and energy productivity in industry. This involves the assessment of current operation and understanding the scope for the extent of exergetic 'improvement potential.'

Thermoeconomics and exergoeconomics, and extended exergy accounting concepts tie the thermodynamic analysis, particularly the exergy analysis, to economy, environment, and sustainability, which has three overlapping elements of economy, environment, and society. The energy type and usage may affect all the three elements. Thermodynamic analysis is also seen as indicating natural limits on the attainment of sustainability. However, the application of such thermodynamic ideas outside the sphere of engineering has its critics. The link between the efficiency of resource utilization, pollutant emissions, and 'exergy consumption' may only be indirect, and generally provide an insufficient basis for environmental appraisal and as appropriate measures of sustainability in and beyond the energy sector [26].

2 Entropy Production

One of the most fundamental outcomes of classical engineering thermodynamics is the idea that the efficiency of a heat engine cannot exceed a certain theoretical limit. For example, the energy conversion efficiency of a heat engine, such as steam power generation, cannot exceed the Carnot efficiency. This limit corresponds to systems that operate reversibly. The difference between the actual and the Carnot work represents the lost work for a heat engine.

The relation of Carnot–Clausius expresses the change of the entropy of a closed system

$$\mathrm{d}S = \mathrm{d}_{\mathrm{e}}S + \mathrm{d}_{\mathrm{i}}S = \frac{\delta_{\mathrm{e}}q}{T} + \mathrm{d}_{\mathrm{i}}S \tag{2.1}$$

Equation (2.1) identifies the two contributions: entropy exchange with the environment $\mathrm{d}S_e$ and entropy change inside the volume under consideration $\mathrm{d}_{\mathrm{i}}S$. The value of $\mathrm{d}_{\mathrm{i}}S$ in every macroscopic region of the system is positive for irreversible changes: $\mathrm{d}_{\mathrm{i}}S > 0$, while it is zero for reversible changes $\mathrm{d}_{\mathrm{i}}S = 0$. The $\mathrm{d}_{\mathrm{e}}S$ may be due to a flow of internal energy, convection entropy flow transported along with the macroscopic flow of the substance as a whole, or the entropy flow caused by diffusion of the individual components. The quantity $\mathrm{d}_{\mathrm{e}}S$ may be positive, negative, or zero in a special case. The rate of entropy production due to irreversibility becomes

$$\mathrm{d}_{\mathrm{i}}S/\mathrm{d}t = \dot{S}_{\mathrm{prod}}. \tag{2.2}$$

For some time entropy production and its minimization estimation have been limited to heat and fluid flow systems [10,27]. The followings are some examples of estimations for the rate of entropy production for various systems:

2.1 Chemical Reactions

For a system, if the change of mole numbers $\mathrm{d}N_k$ is due to irreversible chemical reactions, the rate of entropy production is

$$\dot{S}_{\mathrm{prod}} = \frac{\mathrm{d}_{\mathrm{i}}S}{\mathrm{d}t} = -\frac{1}{T}\sum \mu_k \frac{\mathrm{d}N_k}{\mathrm{d}t} \geq 0 \tag{2.3}$$

where μ_k is the chemical potential.

The rate of entropy production due to electrochemical reactions is

$$\frac{\mathrm{d}_{\mathrm{i}}S}{\mathrm{d}t} = \frac{\tilde{A}}{T}\frac{\mathrm{d}\varepsilon}{\mathrm{d}t} \geq 0 \tag{2.4}$$

where ε is the extent of reaction and $\tilde{A}$ is the electrochemical affinity defined by

$$\tilde{A}_i = A_i + z_i F(\psi_1 - \psi_2) = \tilde{\mu}_1 - \tilde{\mu}_2 \tag{2.5}$$

$$\tilde{\mu}_i = \mu_i + z_i F \psi \tag{2.6}$$

Here z_i is the electrovalency of ionic species i, F is the Faraday number, which is the electrical charge associated with one mole ion of a species with an electrovalence of 1, $\tilde{\mu}_i$ is the electrochemical potential of species i, and ψ_1 is the electrical potential at position 1.

2.2 Mass Diffusion

When a mass diffusion occurs in a system from higher chemical potential μ_2 to lower potential μ_1, we have the rate of entropy production expressed by

$$\frac{\mathrm{d_i}S}{\mathrm{d}t} = -\left(\frac{\mu_2 - \mu_1}{T}\right)\frac{\mathrm{d}N}{\mathrm{d}t} \geq 0 \tag{2.7}$$

where $\mathrm{d}N$ accounts for the change of mass from one region to another.

2.3 Electrical Conduction

The rate of entropy production due to electrical conduction is

$$\frac{\mathrm{d_i}S}{\mathrm{d}t} = \frac{\psi I}{T} \geq 0 \tag{2.8}$$

where ψ is the potential difference and I is the current. The product ψI represents the heat generated. This heat is also called Ohmic heat per unit time. From Ohm's law $\psi = IR$, where R is the resistance.

2.4 Dual-Phase-Lag Heat Conduction

The well-known dual-phase lag heat conduction model, proposed by Tzou [30], introduces time delays to account for the responses among the heat flux vector, the temperature gradient, and the energy transport. Its agreement with experimental results was demonstrated [31]. Recently, the dual-phase lag heat conduction model has been used to interpret the non-Fourier heat conduction phenomena. The one-dimensional dual-phase lag constitutive equation relating heat flux to temperature gradient is expressed as [32]

$$q = \tau_q \frac{\partial q}{\partial t} = -k\frac{\partial T}{\partial x} - k\tau_{\mathrm{T}}\frac{\partial^2 T}{\partial t \partial x} \tag{2.9}$$

where x is the coordinate variable, t the time, q the heat flux, T the temperature, k the thermal conductivity, τ_{T} the phase-lag in the temperature gradient, and τ_{q} the phase-lag in heat flux. Equation (2.9) indicates that the temperature gradient established across a material volume at a position x and time $t + \tau_{\mathrm{T}}$ results in a heat flux at a different instant of time $t + \tau_{\mathrm{q}}$. Equation (2.9) reduces to the hyperbolic thermal wave model by setting $\tau_{\mathrm{T}} = 0$. For situations involving a heat source, such as a laser or microwave with extremely short duration or very high frequency, a very high temperature gradient, and extremely short times, heat is found to propagate at a finite speed. To account for the phenomena involving the finite propagation velocity of the thermal wave, the classical Fourier heat flux model should be modified.

Under the effect of the dual-phase-lag heat conduction the entropy production cannot be described using the classical form of the equilibrium entropy production. Al Nimr et al. [33] investigated the effect of the phase-lags in temperature and in heat flux on the nonequilibrium entropy production. As the difference between τ_{T} and τ_{q} increases, the propagation of the entropy production shifts from the diffusive type to the wavy type. For most practical applications involving the dual phase-lag model, the nonequilibrium temperature may be replaced by the equilibrium temperature [33].

In the absence of the temperature gradient phase-lag ($\tau_{\mathrm{T}} = 0$), the nonequilibrium entropy production S^*_{prod} under the effect of the classical hyperbolic heat conduction model becomes

$$S^*_{\mathrm{prod}}(t, \mathbf{r}) = \frac{e(t, \mathbf{r})}{T(t, \mathbf{r})} + \frac{q^2(t, \mathbf{r})}{kT^2(t, \mathbf{r})} \tag{2.10}$$

where q is the conduction heat flux, e is the energy source per unit volume (W/m^3), $\mathbf{r}$ is the spacial vector.

2.5 Reaction-Transport Systems

Reaction-transport systems represent open and non equilibrium systems with thermodynamic forces of temperature gradient, concentration gradient, and affinity A. For an elementary reaction of S $\rightarrow$ B, the local rate of energy dissipation due to local rate of entropy production is given as the summation of independent flows J and forces X ($\dot{S}_{\mathrm{prod}} = \sum_i J_i X_i$) is

$$T\dot{S}_{\mathrm{prod}} = \mathbf{J}_q \cdot \nabla \ln T - \mathbf{j}_S \cdot (\nabla \mu_S)_{T,P} + J_{\mathrm{r}} A \geq 0 \tag{2.11}$$

where $(\nabla \mu_i)_{T,P} = \sum_{i=1}^{n-1}(\partial \mu_i / \partial w_i)\nabla w_i$, μ_i is the chemical potential of species i, A is the affinity ($A = -\sum \nu_i \mu_i$) and J_r is the reaction rate. Equation (2.11) consists of scalar process of chemical reaction and vectorial processes of heat flow J_q and mass flow J_s, while it excludes pressure, viscous, electrical, and magnetic effects [25,34–37].

3 Balance Equations

Generally the steady-state mass, energy, and entropy balances are used to estimate the rate of entropy production:

Mass balance:

$$\dot{m}_{\text{out}} = \dot{m}_{\text{in}} \tag{3.1}$$

Energy balance:

$$\dot{E}_{\text{out}} = \dot{E}_{\text{in}} \rightarrow \dot{m}_1 H_1 = \dot{q}_{\text{out}} + W_{\text{out}} + \dot{m}_2 H_2 \tag{3.2}$$

Entropy balance:

$$\dot{S}_{\text{in}} - \dot{S}_{\text{out}} + \dot{S}_{\text{prod}} = 0 \rightarrow \dot{m}_1 S_1 - \dot{m}_1 S_2 - \frac{\dot{q}_{\text{out}}}{T_o} + \dot{S}_{\text{prod}} = 0 \tag{3.3}$$

Heat loss from the energy balance:

$$\dot{q}_{\text{out}} = -\dot{W}_{\text{out}} + \dot{m}_1 (H_1 - H_2) \tag{3.4}$$

and the entropy production is:

$$\dot{S}_{\text{prod}} = \dot{m}_1 (S_2 - S_1) + \frac{\dot{q}_{\text{out}}}{T_o} \tag{3.5}$$

The unit amount of energy dissipated:

$$\dot{E}_{\text{loss}} = T_o \dot{S}_{\text{prod}} \tag{3.6}$$

Equations (3.1) to (3.6) can be applied to various processes and devices, such as mixers, nozzles, throttling, turbines, as well as cyclic processes of energy conversion [25].

4 Exergy

Exergy is the maximum amount of work theoretically available by bringing a resource into equilibrium with its surrounding through a reversible process. Therefore, exergy is a function of both the physical properties of a resource and its environment representing a defined state. The thermal state and chemical composition of the natural environment represent a reference state (dead state) for the calculation of exergy.

The environment is composed of large numbers of common species that exist naturally. They are in their stable forms and do not take part in any chemical or physical work interactions between different parts of the environment. We mainly assume that the intensive properties of the environment are unchanging, while the extensive properties can change because of interactions with other systems [6]. There are the components of states differing in their composition or thermal parameters from thermodynamic equilibrium state. These components can undergo thermal and chemical processes. Therefore, they are natural resources with positive exergy. A correct definition of the reference level is essential for the calculation of external exergy losses. Some properties of exergy are [6,25]

- Exergy is measured with respect to the environment; therefore, it is attributed to the composite system. If the environment is a reference state with zero exergy, then exergy becomes a property of the system.
- Exergy decreases due to irreversibilities in the system.
- If a system undergoes a spontaneous change to the dead state without a device to perform work then exergy is completely lost.

4.1 Exergy Loss

The loss of exergy $\dot{E}_{\text{loss}}$ may be estimated based on the temperature of the surroundings of the system T_o

$$\dot{E}_{\text{loss}} = m T_o \left(\frac{\mathrm{d_i} S}{\mathrm{d}t} \right) = (\text{kg})\ (\text{K})\ (\text{kJ/kg s K})\ = \text{kW} \tag{4.1}$$

The rate of loss exergy $\dot{E}x_{\text{loss}}$ represents the overall thermodynamic imperfections and is directly proportional to the rate of entropy production due to irreversibilities in a process [38]. Therefore, exergy loss vanishes in reversible processes. As the exergy loss increases, the net heat duty has to increase for the process to occur. Consequently, smaller exergy loss means less waste heat or thermodynamic imperfections.

4.2 Exergy Flow

In an open system, the specific flow exergy ex_{f} is

$$ex = [h - h_o - T_o(s - s_o)] + \sum_i [\Delta G_i + R T_o c_i \ln(c_i / c_{o,i})] + (1/2)v^2 + gz \tag{4.2}$$

where h and s represent the specific enthalpy and entropy, respectively, at the inlet or outlet; h_o and s_o represent the respective values at the reference state, P_o and T_o show the pressure and temperature of the surroundings. The second term represents the chemical exergy where ΔG is the Gibbs free energy, R is the universal gas constant, c_i is the composition of a species i, and $c_{o,i}$ is the composition of the same species at reference state. The kinetic energy $(v^2/2)$ and potential energy (gz) are relative to the surroundings and contribute fully to the magnitude of exergy. The reference has the temperature $T_o = 298.15$ K and pressure $P_o = 101.325$ kPa. For chemical equilibrium, the mean composition of the earth's atmosphere, the mean composition of seawater, and the mean composition of the earth's crust are taken as the reference state [3]. In an open system, specific flow exergy ex_{f} due to mass flow and flow work is

$$ex_{\text{f}} = \dot{m} \left((h - h_o) - T_o(s - s_o) + \frac{v^2}{2} + gz \right) \tag{4.3}$$

where $\dot{m}$ is the mass flow rate.

4.3 Chemical Energy

The chemical exergy of material substances can be calculated if the pressure P and the temperature T are constant and equal to ambient conditions P_o and T_o

$$Ex = \sum_i n_i(\mu_i - \mu_{io}) \tag{4.4}$$

where μ_i and μ_{io} are the chemical potentials of substance i in its present state and in its environmental state, respectively, and n_i is the number of moles. The chemical potential μ_i is defined in terms of concentration of species ic_i

$$\mu_i = \mu_i^o + RT \ln c_i \tag{4.5}$$

where μ_i^o is the standard state chemical potential. Substitution of Eq. (4.5) into Eq. (4.4) yields

$$Ex = \sum_i n_i(\mu_i^o - \mu_{io}^o) + RT_o \sum_i n_i \ln \frac{c_i}{c_{io}} \tag{4.6}$$

where c_{io} is the concentration of species i at the environmental conditions (dead state). For a single-component system, Eq. (4.6) becomes

$$Ex = n\left(\mu^o - \mu_o^o + RT_o \ln \frac{c}{c_o}\right) = n\left(\Delta G + RT_o \ln \frac{c}{c_o}\right) \tag{4.7}$$

For pure components, the chemical exergy can be obtained by diffusing the components to their reference concentration c_{io} with a partial pressure of P_{io}. For an ideal gas, we obtain

$$Ex = nRT_o \ln \frac{P_i}{P_{io}} \tag{4.8}$$

where P_i and P_{io} refer to the partial pressure of the gas in the emission and in the environment, respectively. Reference temperature is usually taken to be 25 °C (298.15 K), and reference pressure is usually taken to be 101.3 kPa (100 kPa is also common). Reference composition is usually taken to be that of air with some humidity. Besides the major constituents, N_2 and O_2, one has to include minor components that add all the variety of atoms of interest; for chemical reactions involving only C, H, O, and N atoms, the H_2O and CO_2 constituents of air are enough (argon is added in Table 1 to avoid dropping a component more abundant than those retained) [3,4,15]. If a larger variety of atoms is needed, this simple reference environment should be enlarged to include other atoms in the atmosphere (e.g. He), the hydrosphere (dissolved species, but then air should be assumed saturated), and the lithosphere (e.g. one may take SiO_2 as a source of Si), but the problem gets entangled because it becomes unrealistic to assume such a complex system in thermodynamic equilibrium, and thus, no zero exergy level can be ascribed to it [3,15].

For substances in the reference atmosphere, the molar exergy of separation, shown in Table 2, becomes

$$ex_i = -RT \ln x_{i0} \tag{4.9}$$

where R is the universal gas constant, 8.314 J/mol K. For example, for oxygen

Table 1 Molar exergy, ex_i, of pure species relative to a reference atmosphere at $P_0 = 100$ kPa, $T_0 = 25$ °C, and 60 % RH; $ex_i = \mu_i\ (T_0,\ p_0, 1) - \mu_{i0}\ (T_0,\ p_0,\ x_{i0})$ [3,4]

Substance	Formula (state)	Molar fraction in ref. atm. x_i	Molar exergy ex_i, kJ/mol
Nitrogen	N_2 (g)	0.7651	0.66
Oxygen	O_2 (g)	0.2062	3.9
Water	H_2O (l)	0.0190	1.3
Argon	Ar (g)	0.0094	12
Carbon dioxide	CO_2 (g)	0.0003	20
Carbon monoxide	CO (g)	NA	275
Hydrogen	H_2 (g)	NA	236
Methane	CH_4 (g)	NA	831
Ethane	C_2H_6 (g)	NA	1500
Ethylene	C_2H_4 (g)	NA	1360
Acetylene	C_2H_2 (g)	NA	1265
Propane	C_3H_8 (g)	NA	2150
n-Butane	C_4H_{10} (l)	NA	2800
Carbon (graphite)	C (s)	NA	410
Nitrogen monoxide	NO (g)	NA	89
Nitrogen dioxide	NO_2 (g)	NA	56
Ammonia	NH_3 (g)	NA	340
Methanol	CH_3OH (l)	NA	720
Ethanol	CH_3CH_2OH (l)	NA	1400

Table 2 Molar exergy of separation of species in the reference atmosphere at 298 K and 60 % RH (relative humidity) and 100 kPa

Component	Mole fraction x_i	Molar exergy ex_i, J/mol
N_2	0.7651	0.66
O_2	0.2062	3.90
H_2O	0.0190	1.30
Ar	0.0094	12.00
CO_2	0.0003	20.00

$ex_{O_2} = RT \ln x_{O_2} = -(8.314)\cdot(298)\cdot(\ln 0.2062) = 3.9$ kJ/mol.

For water vapor:
$ex_{H_2O} = -RT \ln(\mathrm{RH}) = -(8.314)\cdot(298)\cdot(\ln 0.6) = 1.26$ kJ/mol.

where RH is the relative humidity (partial pressure/saturation pressure at T_o).

Reactions often cause extensive exergy loss. The entropy production can cause the loss of considerable potential work due to a reaction. An electrochemical membrane reactor or a fuel cell could reduce exergy loss considerably. Exergy of a reaction (in its standard state, with input and output at T_o and P_o) is just its Gibbs energy of formation of reaction

$$ex_r = \sum n_i \Delta G^o_{fi} \tag{4.10}$$

where n_i is the molar amounts of species i, which are positive for the products and negative for the reactants. When $ex_r = 818$ kJ/mol, exergy of methane is

$$CH_4 + O_2 \rightarrow CO_2 + 2H_2O$$
$$818 - (2)(3.9) + (2)(1.3) + 1(20) = 831 \text{ kJ/mol } CH_4$$

For a combustion system, the chemical exergy is the maximum theoretical work of a combined system composed of a combustion cell and its surroundings.

4.4 Exergy Balance

The exergy balance for a steady-state system shows the exergy loss

$$\sum_{\substack{\text{into}\\ \text{system}}} \left[\dot{n}Ex + \dot{q}\left(1 - \frac{T_o}{T_s}\right) + \dot{W}_s\right] - \sum_{\substack{\text{out of}\\ \text{system}}} \left[\dot{n}Ex + \dot{q}\left(1 - \frac{T_o}{T_s}\right) + \dot{W}_s\right] = \dot{E}x_{\text{loss}} \tag{4.11}$$

where $\dot{W}_s$ is the shaft work. Exergy balance can also be expressed in exergy rate form

$$\frac{dEx}{dt} = \sum_j \left(1 - \frac{T_o}{T_j}\right)\dot{q}_j - \left(\dot{W} - P_o \frac{dV}{dt}\right) - \dot{E}x_{\text{loss}} \tag{4.12}$$

At absolute temperature T, the exergy transfer accompanying heat transfer becomes

$$Ex_{\text{heat}} = \left(1 - \frac{T_o}{T}\right) q \tag{4.13}$$

Exergy transfer accompanies work

$$Ex_{\text{work}} = W - W_{\text{surr}} \quad \text{(for boundary work)} \tag{4.14}$$

$$Ex_{\text{work}} = W \quad \text{(for other forms of work)} \tag{4.15}$$

The change in exergy of a system can be positive, negative, or zero. When the temperature of a process where heat transfer occurs is less than the temperature of the environment, the transfer of heat and exergy flows in opposite directions. Work and the accompanying exergy transfer can be in the same or opposite directions. We consider the exergy of a change from a given reference state (where exergy is zero); the work attainable in a real process would be [6,38]

$$W = Ex - T_o \Delta S_{\text{total}} \tag{4.16}$$

If the total entropy change vanishes, as in a reversible process, exergy defines an upper limit to the work that is extractable from any process.

4.5 Exergetic Efficiency

Energy supplied by the heat transfer, $\dot{q}_{\text{in}}$, is either utilized, $\dot{q}_u$, or lost to the surroundings, $\dot{q}_l$, and the thermal efficiency, η, is expressed by

$$\eta = \dot{q}_u / \dot{q}_{\text{in}} \tag{4.17}$$

The exergetic efficiency ηth is (exergy recovered)/(exergy supplied)

$$\eta_{\text{th}} = \eta \left(\frac{1 - T_o/T_u}{1 - T_o/T_{\text{in}}}\right) \tag{4.18}$$

Generally, the value of exergetic efficiency is less than unity even when $\eta = 1$. Exergy use would increase as the temperature at the utilization of energy approaches the temperature of inlet energy. The rate of exergy loss accompanying the heat loss $\dot{q}_l$ is $(1 - T_o/T_l)\dot{q}_l$ and depends on the operating temperature. Exergetic efficiency expressions can take different forms; for the following steady-state processes, exergetic efficiency expressions are [25]

- A turbine with adiabatic operation with the work produced $\dot{W}_t$:

$$\eta_{\text{th}} = \frac{\dot{W}_t}{\dot{m}(ex_{f,\text{in}} - ex_{f,\text{out}})} \tag{4.19}$$

- A compressor or pump with work input $\dot{W}$ and adiabatic operating conditions

$$\eta_{\text{th}} = \frac{\dot{m}(ex_{\text{f,out}} - ex_{\text{f,in}})}{(-\dot{W})} \tag{4.20}$$

- A heat exchanger at adiabatic conditions with both streams at temperatures above T_o

$$\eta = \frac{\dot{m}_{\text{c}}(ex_{\text{f,out}} - ex_{\text{f,in}})_{\text{c}}}{\dot{m}_h(ex_{\text{f,in}} - ex_{\text{f,out}})_h} \tag{4.21}$$

where $\dot{m}_{\text{c}}$ and $\dot{m}_h$ represent the mass flow rates of cold and hot streams, respectively.

- For an adiabatic chemical reaction at constant pressure, the enthalpy remains constant. The loss in exergy is given by the exergy of reactants ex_1 and the exergy of the reaction products ex_2

$$W_l = ex_1 - ex_2 = T_0(s_1 - s_2) \tag{4.22}$$

and

$$\eta_{\text{th}} = 1 - \frac{W_l}{ex_1} = 1 - \frac{T_0(s_1 - s_2)}{ex_1} \tag{4.23}$$

For a combustion reaction taking place in a well-insulated chamber with no work produced, exergetic efficiency becomes

$$\eta_{\text{th}} = 1 - \frac{Ex_{\text{loss}}}{Ex_{\text{F}}} \tag{4.24}$$

where Ex_{F} is the rate of exergy entering with the fuel, and Ex_{loss} is the exergy loss. The exergy efficiency by the second law is

$$\eta_{\text{th}} = \frac{Ex_{\text{out}}}{Ex_{\text{in}}} \tag{4.25}$$

Intrinsic efficiency η_{in} takes into account the transiting exergy Ex_{tr}

$$\eta_{\text{in}} = \frac{Ex_{\text{out}} - Ex_{\text{tr}}}{Ex_{\text{in}} - Ex_{\text{tr}}} = \frac{Ex_{\text{p}}}{Ex_{\text{c}}} \tag{4.26}$$

The transiting exergy is the part of the exergy entering a unit operation; it traverses without undergoing any transformation and exergy loss. The terms Ex_{c} and Ex_{p} are the exergies actually consumed and produced, respectively.

5 Thermodynamic Analysis

Thermodynamic analysis is popular in evaluating the efficiency and improving the thermodynamic imperfections of mainly thermal engineering systems. Thermodynamic analysis mainly consists of three parts: the first part assesses the thermodynamic performance of the current operation. The second part identifies the scope of improvements and retrofits to reduce the cost of operation. The third part involves the assessment of the thermodynamics and economic effectiveness of the retrofits. Second law analysis can identify the sources and quantity of entropy production in various processes in a system. Exergy analysis describes the maximum available work when a form of energy is converted reversibly to a reference system in equilibrium with the environmental conditions; hence, it can relate the impact of energy utilization to environmental degradation. Pinch analysis can reduce the hot and cold utility requirements by integrating process heat streams. On the other hand, the equipartition principle states that a process would be optimum when the thermodynamic driving forces are uniformly distributed in space and time. Thermodynamic analysis aims at identifying, quantifying, and minimizing irreversibilities in a system. Such analysis is of considerable value when efficient energy conversion is important. This chapter briefly discusses the following methodologies of thermodynamics analysis and provides some examples:

- Second law analysis,
- Exergy analysis,
- Pinch analysis,
- Equipartition principle,
- Gibbs free energy minimization,
- Thermoeconomics,
- Exergoeconomics,
- Extended exergy analysis.

5.1 Second Law Analysis

The product of thermodynamic forces and flows yields the rate of entropy production in an irreversible process. Transport phenomena and chemical reactions are nonequilibrium phenomena and are irreversible processes. Second law analysis can determine the level of energy dissipation from the rate of entropy production in the system [25,28]. The map of the volumetric entropy production rate identifies the regions within the system where excessive entropy production occurs due to irreversible processes [39–53].

In every non equilibrium system, an entropy effect exists either within the system or through the boundary of the system. For a general steady-state flow process, the rate of entropy production becomes

$$\dot{S}_{\text{prod}} = \sum \dot{m}_{\text{out}} s_{\text{out}} - \sum \dot{m}_{\text{in}} s_{\text{in}} - \frac{\dot{q}_o}{T_o} - \sum \frac{\dot{q}_i}{T} \tag{5.1}$$

Researchers and engineers extensively utilized second law analysis in the field of heat and fluid flow as well as laser applications [42,43,45]. Bejan [10,27] developed the basic approach, methodology, and applications. For an incom-

pressible flow in a heat and fluid flow system, the rate of entropy production is

$$\dot{S}_{\text{prod}} = \frac{k}{T^2}(\nabla T)^2 + \frac{\mu}{T}\Theta \tag{5.2}$$

where μ is the viscosity and Θ is the viscous dissipation function (in s^{-2}). For a two-dimensional Cartesian coordinate system, Eq. (5.2) can be expressed as

$$\dot{S}_{\text{prod}} = \frac{k}{T^2}\left[\left(\frac{\partial T}{\partial x}\right)^2 + \left(\frac{\partial T}{\partial y}\right)^2\right] + \frac{\mu}{T}\left\{2\left(\frac{\partial v_x}{\partial x}\right)^2 + 2\left(\frac{\partial v_y}{\partial y}\right)^2 + \left(\frac{\partial v_x}{\partial y} + \frac{\partial v_y}{\partial x}\right)^2\right\} \tag{5.3}$$

Equation (5.3) shows that the local irreversibilities are due to heat and viscous effects. Entropy production is positive and finite as long as temperature and velocity gradients exist, as shown

$$\dot{S}_{\text{prod}} = \dot{S}_{\text{prod},\Delta T} + \dot{S}_{\text{prod},\Delta P} \tag{5.4}$$

while the irreversibility distribution ratio is

$$\text{Be} = \dot{S}_{\text{prod},\Delta T}/\dot{S}_{\text{prod}} \tag{5.5}$$

and is called the Bejan number Be. Be = 1 is the limit at which all irreversibility is due to heat transfer only. Irreversibility due to heat transfer dominates when $\text{Be} \gg \frac{1}{2}$, while $\text{Be} \frac{1}{2}$ indicates that irreversibility due to friction dominates. Suitable trade-offs between the use of energy and capital may be required by identifying and eliminating design parameters and operating conditions that cause excessive entropy production.

5.2 Exergy Analysis

The exergy method has been widely used for the analysis of industrial processes and energy productions [54–72,74–78]. They include power cycle operations, biomass and coal gasification, solar energy applications, refrigeration, waste heat utilization, and distillation column systems. Exergy analysis is conducted to save the initial and operational costs of mainly thermal engineering systems. The main steps of exergy analysis are as follows:

- Define the system boundary of processes to be analyzed.
- Define all the assumptions and the reference temperature, pressure, and composition.
- Consider possible heat recovery and heat integration strategies for all the processes analyzed.
- Determine the total exergy losses.
- Determine the thermodynamic efficiency.
- Use exergy loss profiles to identify the regions performing poorly.
- Identify improvements and modifications to reduce the cost of energy and operation.

Exergy analysis firstly identifies the processes that contribute toward to the total exergy loss. Second, it identifies the scope for optimization either by increasing the conversion efficiency by reducing the irreversibility or reducing the cost of operation [10,27]. The second part is the one mainly left open without clear methodologies in many publications. This may lead to incomplete exergy analysis. Thermodynamics, fluid mechanics, heat and mass transfer, kinetics, material properties, operational and design constraints, and geometry are required to establish the relationships between physical configuration and entropy production. These relationships are vital to minimize entropy production.

Exergy analysis for the following systems has attracted a great deal number of researchers:

- Power cycle applications
- Biomass and coal gasification
- Solar energy applications
- Refrigeration applications
- Waste heat utilization applications
- Distillation column systems
- Heat and fluid flow in microchannels

These systems are briefly discussed in the following sections.

5.2.1 Power Cycle Applications

As the power cycles convert a large amount of thermal energy to mainly electricity at relatively low efficiency, they have been subject to extensive exergy analyses [54–77]. An increase in efficiency may lead to savings in fuel costs and minimize adverse environmental effects. The two basic approaches in increasing the thermal efficiency of a cycle are (i) design a process that transfers heat to the working fluid at high temperature in the boiler and (ii) design a process that transfers heat to the working fluid at low temperature in the condenser. These may decrease the temperature differences, and hence the level of irreversibility. The highest exergy losses or the work losses are in the boiler and condenser, respectively.

The followings are only a small number of relatively recent examples of such collective efforts for exergy analysis. Exergy analysis has been carried out for various designs [55,58–61], such as for the effect of 'n' number of feed water heaters on performance of a steam power cycle, for possible improvements in efficiency with increases in boiler pressure, turbine inlet temperature, and furnace temperature [55]. Exergy analysis for a coal-based power and methanol systems shows that polygeneration system may save 3.9 and 8.2 % energy com-

pared with the individual processes. Synergetic integration of the power production system and the chemical production in polygeneration may be promising with a right ratio of capacity ratio of chemical process to power production system [56]. A conceptual trigeneration system proposes the conventional gas turbine cycle for the high temperature heat addition while adopting the heat recovery steam generator for process heat and vapor absorption refrigeration for the cold production. That exergy loss in a combustion chamber is significantly affected by the pressure ratio and turbine inlet temperature [67,73].

To find out the contributions of different parts of a plant towards exergy losses, the entire steam power plant cycle may be split up into three zones for the analysis: (1) only the turbo-generator with its inlets and outlets, (2) turbo-generator, condenser, feed pumps and the regenerative heaters, and (3) the entire cycle with boiler, turbo-generator, condenser, feed pumps, regenerative heaters, and the plant auxiliaries. The load variation studies with the data at 100, 75, 60 and 40 % of full load shows that the major source of irreversibility in the power cycle is the boiler, which contributes to exergy losses of the order of 60 % [71,72].

Trigeneration with gas turbines can improve energy utilization. Introducing air refrigeration cycle for inlet air cooling provides considerable improvement in the performance. Inlet air cooling increases the energy and exergy efficiencies [66,72]. An exergy analysis is also used to compare the thermodynamic performance and emission of CO_2 from different types of lignites at various ambient temperatures [69].

Among the various designs of power production cycles, reheat, regenerative, cogeneration, as well as combined cycles are often analyzed based on exergy for possible improvements [47,58,61,70,71]. Such improved designs can meet the growing energy demand and hence needs to be optimized by identifying the irreversibility at each component. Energy and exergy analyses for a combined-cycle power plant by using the data taken from its units in operation are used to analyze a complex energy system more thoroughly and to identify the potential for improving efficiency of the system. Some constructive and thermal suggestions for these devices have been made to improve the efficiency of the system [64].

Table 3 compares the exergy losses of ideal and actual reheat Rankine cycle operations. The total exergy loss increases from 1417.2 to 1673.55 kJ/kg in the actual operation. This shows an increase of 18.0 % in the actual operation. In this actual reheat Rankine cycle, the steam expands in two stages. In the first stage, the steam expands to 4350 kPa and is sent to the reboiler where it is reheated at constant pressure to 823.15 K. In the second stage, the steam expands and the discharged steam at 10 kPa is sent to the condenser. The exergy losses or the work losses are 72.8 and 9.2 % in the boiler and condenser, respectively. The exergy loss in the reheating step is low (2.9 %). Reheating reduces the moisture in the turbine [25].

Table 3 Distribution of exergy losses in actual and ideal reheat Rankine cycles

Process	Actual reheat Rankine		Ideal reheat Rankine	
	Ex_{loss} (kJ/kg)	%	Ex_{loss} (kJ/kg)	%
2–3	1212.54	72.4	1220.89	86.1
3–4	19.57	1.2	0	0
4–5	48.41	2.9	59.00	4.2
5–6	238.50	14.3	0	0
6–1	154.10	9.2	137.31	9.7
Cycle	1673.55		1417.20	

Thermodynamic analyses of Otto cycle (spark-ignition engines) with various gas mixtures as working fluids with variable temperature specific heats [59,60] shows that the exergy loss during the combustion process decreases as the engine load or engine speed increases. Exergy analysis is also helping to understand the performance of hybrid power systems, such as gas turbine cycle with steam generation for methane conversion within solid oxide fuel cells [75,76].

5.2.2 Biomass and Coal Gasification Applications

Based on exergy consumptions, the annual renewable energy resource utilization may be improved and optimized toward effective energy-efficiency delivery mechanisms [78–91]. Thermodynamic performances based on hydrogen yield and exergy efficiency of five different biomass processes show that the hydrogen yield is around 0.097 kg/kg dry biomass, while the exergy efficiency is around 50 % without heat recovery and around 64 % with heat recovery [78].

Exergy analysis is performed for a hybrid plant producing heat and power from biomass by the use of a two-stage gasification concept, solid oxide fuel cells and micro gas turbine [79] with a combined zero-dimensional component model into the complete system-level models. Optimization leads to a gain of 6 % in the electrical efficiency of the plant producing 290 kW at efficiency of 58.2 % based on lower heating value [79]. The combination of fuel cells with conventional mechanical power generation technology promotes effective transformation of chemical energy to electricity. Exergy analysis of a gas turbine cycle with steam generation for methane conversion within solid oxide fuel cells shows that exergy losses throughout the process attributable to fuel combustion are reduced by about 50 % [74].

The feasibility study of a demonstration plant producing hydrogen and benzene from biogas shows that only 21 % of the input exergy is converted to hydrogen and benzene, while the rest is consumed [80]. Gasification with air, steam, and

mixed air-steam is performed to find the optimum equivalence ratio, steam to biomass ratio, and operating temperature to maximize the yield of hydrogen production with low energy consumption. With the obtained optimum operating conditions, the efficiency may be as high as 65 % [81–83].

Thermodynamic analysis based on energy and exergy analyses of a coal gasification and split Rankine combined cogeneration plant may be used for the optimization of the operation [82,83]. The exergy analysis shows that the maximum exergy losses occur in the gasifier and the steam turbine. An air-blown gasification for integrated gasification combined cycle application at various gasification temperatures (oxygen-blown and air-blown) shows that the largest exergy losses (about 30 %) are associated with the processes where chemical reactions occur. The exergy analysis showed a potential improvement in the net plant efficiency with respect to the oxygen-blown case [84].

Hydrogen production from gasification of biomass, coal, and natural gas is another important process analyzed by means of exergy [78,85–89,91,92]. This combined system uses the high-temperature gas flow from the turbine to heat the input flows of natural gas and air, and generate high pressure steam, which is mixed with natural gas at the solid oxide fuel cell stack inlet to facilitate its conversion [88].

Thermodynamic potential analysis study on solid oxide fuel cells and micro gas turbine hybrid power system shows that the turbine inlet temperature is a key parameter that limits the efficiency of hybrid power system [75]. Integration of a near atmospheric solid oxide fuel cell with allothermal biomass gasification into a combined heat and power system may be evaluated in exergy terms [74].

5.2.3 Solar Energy Applications

Exergy analysis can provide some methods to save cost and keep the efficiency of domestic and industrial solar energy utilization high by taking into account the related exergy losses [93–106]. Thermal energy storage is an integral part of solar energy utilization, and the thermal behavior of particle dispersed phase changing material unit in terms of the total exergy recovered may lead to better designs [95,96,102,104]. The solar energy applications through the combination of photovoltaic and thermal systems are studied with the help of energy and exergy analyses [98,105].

Exergetic analysis has become an integral part of the thermodynamic assessment of a parabolic trough solar thermal plant with modern combined cycle power plants. Energy and exergy analyses for the solar field and combined cycle are carried out to identify the primary exergy losses in combustor, collector, heat exchangers, and pumps in the operation [97,100]. In another industrial solar energy application, exergy analysis is performed of a solar power tower system using molten salt as the heat transfer fluid [100,106]. Maximum exergy loss occurs in the receiver system, although main energy loss occurs in the power cycle system. Overall energy and exergy efficiencies of the solar tower system can be increased by integrating advanced power cycles. Exergy analysis is developed to assess a Rankine cycle system by using CO_2 as working fluid and powered by solar energy to optimize and improve the system [96].

5.2.4 Waste Heat Utilization Applications

Low-quality thermal energy demands in buildings are mainly satisfied with high-quality sources (e.g. natural gas fired in condensing boilers). Exergy analysis, pursuing a matching in the quality level of energy supplied and demanded, suggests the necessity of substituting high-quality energy sources by other low-quality energy flows, such as waste heat [107–111]. Results of dynamic energy and exergy analyses of the waste-heat-based district heating systems show that lowering supply temperatures from 95 to 57.7 °C increases the final exergy efficiency of the systems from 32 to 39.3 % [107]. Exergy analysis of a geothermal district heating system with actual system data shows that the exergy losses in the system, particularly due to the fluid flow, take place in the pumps and the heat exchanger, as well as the exergy losses of the thermal water (e.g. geothermal fluid) and the natural direct discharge of the system [107–110].

Using the actual thermal data, energy and exergy evaluation, and modeling of geothermal district heating systems may be performed for their system analysis, performance evaluation, and optimization at various reference temperatures [110]. Studies show how energy and exergy efficiencies of the heating system will change with the reference temperature and how exergy losses will be affected by the temperature difference between the geothermal resource and the supply temperature of the district heating distribution network [109,110].

The feasibility of plants for zero carbon building complex with respect to conventional plants is investigated for the following two plants [111]: the first plant is composed of air-to water heat pumps for space heating and cooling, photovoltaic solar collectors, air dehumidifiers, thermal solar collectors, and a wood pellet boiler for water heating supply; in the second, the air-to-water heat pumps are replaced by ground-coupled heat pumps. The exergy analysis confirms the feasibility of both plants and shows that the ground coupled heat pumps yield a higher exergy saving.

5.2.5 Refrigeration Applications

The combined production of power, heat, and refrigeration has been analyzed by means of exergy [67,73,112–115]. Exergy analysis is performed for absorption refrigeration machines by splitting the exergy loss into endogeneous/

exogeneous and unavoidable/avoidable parts [24] and by using lithium bromide and water as the working fluids [113]. An optimization procedure has been applied to a lithium-bromide absorption cycle that consists of determining the enthalpy, entropy, temperature, mass flow rate, and heat rate in each component [24]. Thermodynamic analysis may be used for cascade refrigeration system using ozone-friendly refrigerants to optimize the design and operating parameters of the system [114,115].

5.2.6 Distillation Column Systems

Distillation column systems are highly energy intensive and hence studied by exergy analysis [116–123]. In a distillation column, we supply heat at a higher temperature source in the reboiler and then discharge at a lower temperature in the condenser (Fig. 1). Assuming the column to be a reversible heat engine, the net work available from the thermal energy is

$$W_{\text{heat}} = q_R\left(1 - \frac{T_o}{T_R}\right) - q_C\left(1 - \frac{T_o}{T_C}\right) \tag{5.6}$$

where T_o is the ambient temperature. The temperature corrections describe the maximum fraction of theoretical work extracted from thermal energy at a particular ambient temperature.

The minimum separation work $W_{\min}$ required for separation is the net change in availability $A \quad (A = H - T_o S)$

$$-W_{\min} = \Delta A_s = A_{\text{prod}} - A_{\text{feed}} \tag{5.7}$$

The change of availability of separation is the difference between the work supplied by the heat and the work required for separation, which contains the work lost due to irreversibilities

$$\Delta A_s = W_{\text{heat}} - W_{\text{ts}} \tag{5.8}$$

where W_{ts} is the total work necessary for the separation. Minimizing the work lost due to irreversibility will minimize the total heat needed for separation. Efficiency based on the second law of thermodynamics is

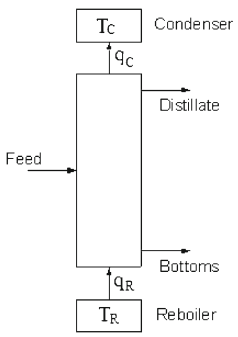

Fig. 1 Distillation column as a heat engine between reboiler and condenser

$$\eta_{\text{th}} = \frac{W_{\min}}{W_{\min} + W_{\text{lost}}} \tag{5.9}$$

For example, propylene–propane mixture is a close boiling mixture and requires a distillation column with a reflux ratio of 15.9 (close to minimum) and 200 equilibrium stages are necessary [25,122]. The reboiler and condenser duties are 8274.72 and 8280.82 kW, respectively. The reference temperature is 294 K. The lost work is obtained from as $\dot{W}_{lost} = T_0 \dot{S}_{\text{prod}} = 1902.58$ kW [108]. Availability $A_i = H_i - T_0 S_i$ analysis yields

$$\dot{W}_{\min} = \sum_{\text{out}} \dot{n} A - \sum_{\text{in}} \dot{n} A = 140.81 \text{ kW}$$

The thermodynamic efficiency η_{th} is 0.0689 or 6.89 %

- The work lost due to a high-pressure drop (as high as 10 psi) is considerable at the condenser and reboiler.
- The work lost due to heat transfer results from differences in temperature between the inlet streams of liquid and vapor on each tray and is a large contributor to the total lost work.
- Large amounts of lost work due to mixing and mass transfer mainly occur around the feed trays. The mixing may take place between streams with widely different compositions.

Exergy analysis is used in designing thermodynamically optimum columns and assessing the performance of existing columns [17–20,119–123] in the following stages: (i) the assessment of the status of exergy use, (ii) if necessary, the modification and improvement of the operation to reduce irreversibility and hence the cost of energy, and (iii) the assessment of the thermodynamic and economic effectiveness of the retrofits. The retrofits involve the feed conditioning (heating or cooling), adjusting the reflux ratio, adjusting the feed stage location, using side heating and cooling, and the uniform distribution of the entropy production over the column volume [19,25].

One of the outcomes of thermodynamic analysis of distillation columns is the stage exergy loss profiles generated by the Aspen Plus simulator [122]. The converged mass and heat balances and the exergy loss profiles produced by the Aspen Plus simulator can help in assessing the thermodynamic performance of distillation columns. The exergy values are estimated from the enthalpy and entropy of the streams generated by the simulator. The exergy loss of stage i

$$\dot{E}x_{\text{loss},i} = \dot{E}x_{i+1}^V + \dot{E}x_{i-1}^L - \dot{E}x_i^V - \dot{E}x_i^L + \dot{q}\left(1 - \frac{T_o}{T_i}\right) \tag{5.10}$$

where $\dot{E}x_{i+1}^V$ and $\dot{E}x_{i-1}^L$ are the rates of the exergy of vapor and liquid phases for stages $i+1$ and $i-1$, respectively. As

an extensive property, exergy loss can be used in the sensitivity analysis and optimization of distillation columns. The difference between the exergies of products and feed streams of a column determines the minimum amount of exergy for a required separation work

$$\dot{E}x_{\text{sep}} = \sum_{\text{products}} (\dot{E}x) - \sum_{\text{feeds}} (\dot{E}x) \tag{5.11}$$

For a reversible operation, the net exergy from heat is

$$\dot{E}x_{\text{heat}} = \sum_{\substack{\text{into}\\ \text{system}}} \dot{q}_R \left(1 - \frac{T_o}{T_H}\right) - \sum_{\substack{\text{out of}\\ \text{system}}} \dot{q}_C \left(1 - \frac{T_o}{T_C}\right) \tag{5.12}$$

where $\dot{q}_R$ is the heat absorbed in the reboiler, and $\dot{q}_C$ is the heat discharged in the condenser. As the exergy loss increases, the net heat exergy has to increase to enable the column to achieve the required separation. Supplying more heat increases the temperature in the reboiler and hence the net heat exergy. However, the temperature of the reboiler is limited to avoid product thermal degradation, while the temperature of the condenser is set by cooling utilities.

The unavoidable part of the total exergy loss $Ex_{\text{loss,un}}$ is

$$Ex_{\text{loss,un}} = \sum_{i=1}^{N} \left(\frac{T_o}{T_i}\right) Ex_{\text{loss},i} \tag{5.13}$$

where N is the number of stages including the condenser and reboilers, and T_i is the temperature of stage i. A quantified potential improvement indicator (PI) is

$$PI = \frac{Ex_{\text{loss}} - Ex_{\text{loss,un}}}{Ex_{\text{loss}}} \tag{5.14}$$

The indicator PI represents exergy losses that are avoidable because of the configuration of that column and the transport rate limitations. The difference between the net exergy of heat and the exergy of separation represents the total exergy loss in the column [120–122]

$$\dot{E}x_{\text{loss}} = \dot{E}x_{\text{heat}} - \dot{E}x_{\text{sep}} \tag{5.15}$$

The total exergy losses consist of column configuration limitations due to the design and transportation limitations. For $\dot{E}x_{\text{sep}} > 0$, the exergy efficiency of column i becomes

$$\eta_i = \frac{\dot{E}x_{\text{sep},i}}{\dot{E}x_{\text{heat,i}}} = \frac{\dot{E}x_{\text{sep},i}}{\dot{E}x_{\text{loss,i}} + \dot{E}x_{\text{sep},i}} \tag{5.16}$$

The values of efficiencies help in assessing the effectiveness of exergy usage, as the value of $(1-\eta)$ is directly related to the exergy loss. They can be used to compare the performance of columns with each other. Smaller exergy losses mean the utilization of a higher portion of available energy and hence fewer thermodynamic imperfections in a column [122].

The following examples illustrate the use of exergy in the separation sections of a methanol production plant. The column stages are numbered starting from the condenser. The rate of entropy production, the stream exergy flows, the total exergy losses of the columns, the minimum values of separation exergy, and the thermodynamic efficiencies are estimated.

Case Study: Assessment of separation of methanol plant

Figure 2 shows the separation section of a methanol plant producing 62,000 kg/h and 99.95 % pure methanol from natural gas, carbon dioxide, and water as the basic feed streams. The methanol synthesis takes place in a tube-cooled reactor with an exit temperature of 240 °C. The output is flashed and the liquid stream 407 is fed to the separation section where the methanol is purified in two distillation columns. The first column has 51 stages, a partial condenser at the top, and a side condenser at stage 2. It receives a side heat stream of 15.299 MW at stage 51 and operates without a

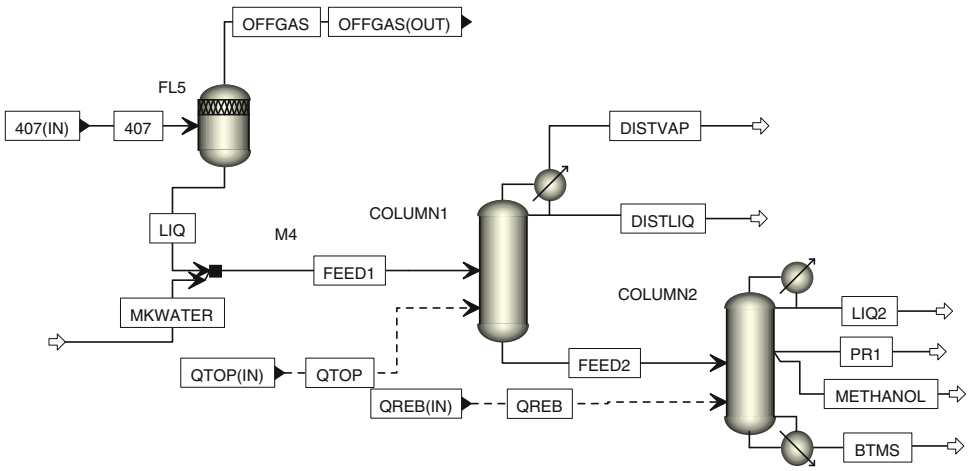

Fig. 2 Separation section of the methanol plant

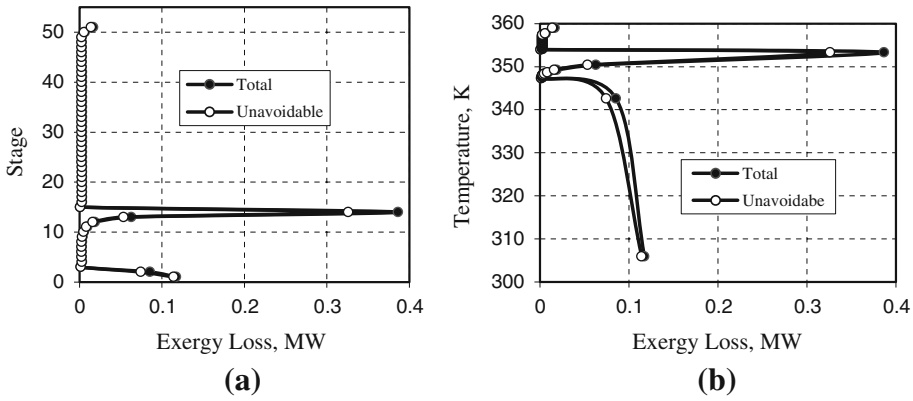

Fig. 3 Exergy loss profiles of column 1. **a** Stage-exergy loss, **b** temperature-exergy loss [122]

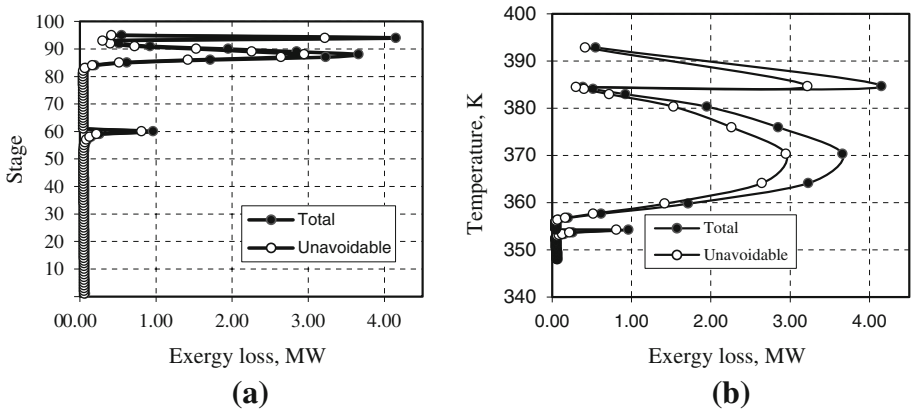

Fig. 4 Exergy loss profile of column 2. **a** Stage-exergy loss, **b** temperature-exergy loss [120]

reboiler. The feed enters at stage 14. The second column has 95 stages and a total condenser. It receives a side heat stream of 18.9 MW at stage 95 as a part of a reboiler duty of 282.283 MW, and operates with a very high reflux ratio. The feed enters at stage 60. The methanol is a side product drawn from stage 4. Converged mass and energy balance data from Aspen Plus are the result of the thermodynamic methods of Redlich–Kwong–Soave for vapor properties, and the activity coefficient model of NRTL and Henry components method for the equilibrium and liquid properties.

Figures 3 and 4 display the exergy loss profiles together with the unavoidable portion of the exergy loss for columns 1 and 2, respectively. Figure 3 shows that the main exergy losses are 0.367 MW (44 %) at the feed stage and 0.117 MW (14 %) at the condenser of column 1. The large exergy losses are due to mass transfer and mixing occurring at the feed stage, where streams at different compositions and temperatures are mixed. Figure 4 shows that column 2 operates with rather large exergy losses at the feed stage and at stages close to the reboiler. The losses occur mainly because of the feed stage and heat transfer and pressure drops (as high as 8–10 psi) in the vicinity of the reboiler. The temperature-exergy profile in Fig. 5 displays large amounts of exergy losses mainly due to the heat transfer between the stages at 355 and 393 K and contributes a large part of the total loss.

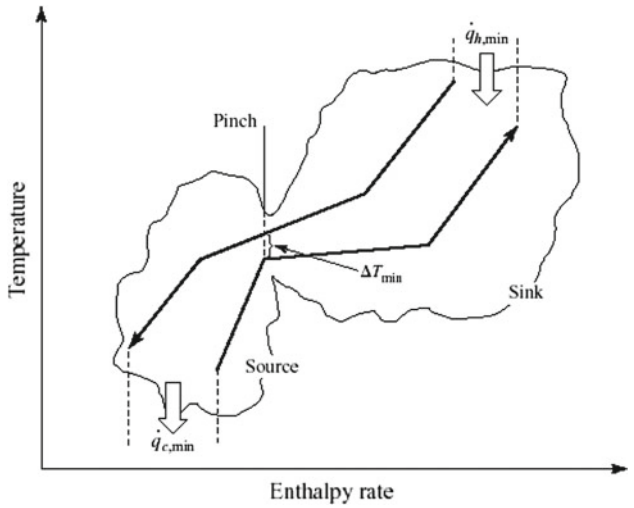

Fig. 5 Hot and cold composite curves

Table 4 shows that column 2 operates with efficiency as low as 4.1 %, while the efficiency of column 1 is 50.6 %.

The exergy values for the whole separation system of two columns are also low and need to be improved. The individual values of PI show that it is possible to reduce by 13.1 % the total loss of 0.834 MW in column 1 and by 19.1 % the total loss of 27.813 MW in column 2. Despite the heat integration, the separation section of the methanol plant performs poorly in utilizing the exergy in the distillation columns.

Al Muslim et al. [119] performed the exergy analysis of single- and two-stage crude oil distillation. The single-stage system consists of a crude heating furnace and a 27-tray atmospheric distillation column. The two-stage system consists of a furnace, a 13-tray atmospheric distillation column, another furnace to heat the bottom product of the first unit, and a second distillation column with 14 trays. Table 5 compares the exergy analysis of the systems and shows considerable reduction in exergy losses.

Case Study: Refinery Operation Optimization by Exergy Analysis

Rivero [17,18] reported exergy analysis for an existing refinery operation. Table 6 shows the considerable economic gains due to the reduction in exergy losses after the optimization.

5.2.7 Heat and Fluid Flow in Microchannels

Microchannel heat sinks, such as a microchannel of square cross section with internal longitudinal fins, are an integral part of most devices used for thermal management in electronic equipment cooling. A thermodynamic analysis may help optimize the height of fin and thermophysical parameters, based on the minimizing the entropy generation rates due to heat transfer and fluid flow within the microchannel [124,125].

Table 4 Results of exergy analysis for the section shown in Fig. 2

	$\dot{S}_{prod}$ (MW/K)	$\dot{E}x_{sep}$ (MW)	$\dot{E}x_{heat}$ (MW)	$\dot{E}x_{loss}$ (MW)	$\dot{E}x_{loss,un}$ (MW)	η %	$\dot{E}x_{reduced}$ (MW)	PI (%)
Column 1	0.00217	0.856	11.690	0.834	0.724	50.6	0.110	13.1
Column 2	0.0890	1.135	28.114	26.979	21.810	4.1	5.169	19.1
Columns 1+2	0.0912	1.991	29.804	27.813	22.535	6.6	5.279	18.9

Table 5 Exergy analysis for single-stage- and two-stage crude oil distillation systems [119]

System	Exergy input (MW)	Exergy output (MW)	Overall exergy loss (MW)	Overall exergy efficiency (%)	Column exergy losses (MW)
Single-stage	498.8	69.8	429.0	14.0	137.2
Two-stage	352.0	110.9	241.1	31.5	121.6
% Difference	29.4	58.8	43.8	125	11.4

Reproduced with permission

Table 6 Exergy analysis and loss reduction in a modified refinery [17,18]

Unit	Exergy loss before optimization (%)	Exergy loss after optimization (%)	Proposal investments ($1000)	Payback time (months)	NPV[b] 10 years of investments
Combined distillation unit	20.4	17.2	2822.3	17	7.37
Naphtha HDS unit	3.2	2.7	1101.2	69	1.80
Naphtha reforming unit	10.9	7.9	1204.8	5	3.98
HDS[a] unit	3.4	2.8	834.0	53	2.04
Catalytic cracking unit	19.5	12.7	7822.0	3	47.4
Visbreaking unit	2.9	3.7	1000.0	3	33.27
Utilities plant	39.8	36.7	660.6	4	32.19
Total	100.0	84.3	15245.0	5	24.48

Reproduced with permission
[a] HDS: Hydrodesulphurization
[b] NPV: Net present value of operating cost

Entropy generation of forced convection heat transfer of liquid fluid over the horizontal surface with embedded open parallel microchannels at constant heat flux boundary conditions may be formulated by an integral of the local entropy generation. Embedded open parallel microchannels within the surface can sufficiently reduce both friction and thermal irreversibilities of liquid fluid through slip-flow conditions [125].

5.3 Pinch Analysis

Pinch analysis optimizes systems with their utilities using the principles of thermodynamics. Temperature-enthalpy diagrams called the composite curves represent the thermal characteristics of hot and cold streams (Fig. 5). Hot and cold streams can only exchange energy up to a minimum allowable temperature difference $\Delta T_{\min}$. The temperature level at which $\Delta T_{\min}$ is observed in the system is called the pinch point or pinch condition, which defines the minimum driving force and hence the minimum entropy production allowed in a network. Above the pinch, only the hot utility is required, while only the cold utility is required below the pinch, and no heat should be transferred across the pinch [25]. An increase in $\Delta T_{\min}$ causes higher energy costs and lower capital costs. Consequently, an optimum $\Delta T_{\min}$ exists where the total annual cost is minimized (Fig. 6). Once the $\Delta T_{\min}$ is chosen, minimum hot and cold utility requirements can be evaluated from the composite curves. Pinch analysis has been applied widely in industry leading considerable savings.

Pinch analysis can specify the exchanged heat and mass between hot/rich and cold/lean streams. According to the second law of thermodynamics [122–127]:

$$\begin{pmatrix}\text{heat/mass lost by hot/rich streams}\\ \text{below the pinch point}\end{pmatrix} - \begin{pmatrix}\text{heat/mass gained by cold/lean streams}\\ \text{below the pinch point}\end{pmatrix} \leq 0 \quad (5.17)$$

Pinch analysis is well-established tool in designing an efficient heat exchanger network [25,129]. Pinch analysis has also been extended to the integration of chemical reactor systems with heat exchangers, optimization of industrial ammonia plant, and nitric acid plant. For example, column grand composite curves can be used to modify the column and heat exchanger network; a possible modification is the use of heat pumps in columns by identifying the heat sinks and sources, leading to considerable saving and a shorter payback period [25,122,123].

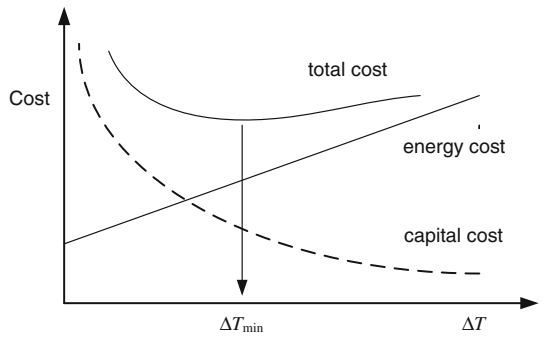

Fig. 6 Optimum $\Delta T_{\min}$ from energy cost and capital cost changes

Case Study: Pinch analysis: Column Grand Composite Curves: $T - H$, or Stage-H

The column grand composite curves ($T - H$; Stage-H) for a five-component mixture have been obtained using the Aspen Plus column-targeting tool capability for thermal analysis. This analysis is helpful in identifying the targets for appropriate modifications to reduce utility and capital costs, improve energy efficiency, and facilitate column debottlenecking. The column grand composite curves (Fig. 7) are based on the practical near-minimum thermodynamic condition approximation and show the theoretical minimum heating and cooling duties within the temperature range. The stage-enthalpy calculations take into account the losses or inefficiencies stemming from the actual column design, such as pressure drops, and multiple-side products. Figure 7 can be useful for identifying the targets for feed conditioning and location, reflux ratio, and heat integration modifications. For example, the column grand composite curves indicate distortions as significant projections around feed stage location (pinch point) if the current feed stage is inappropriate. Besides, a feed stage too high up or too low in the column will display sharp enthalpy changes on the condenser and on the reboil-

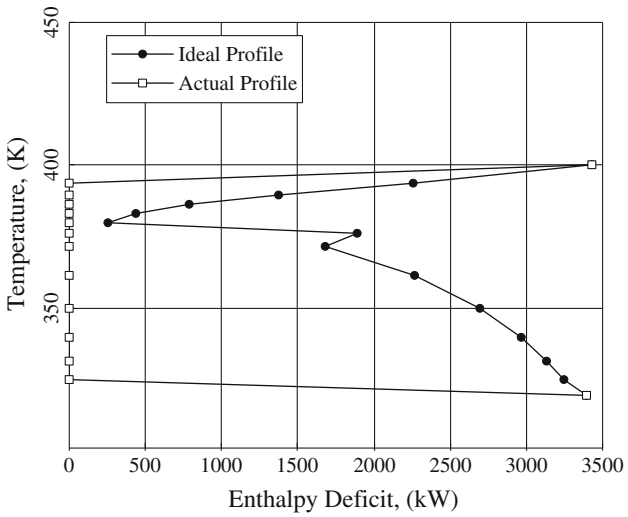

Fig. 7 Column grand composite curve of temperature enthalpy obtained from the simulations with the Aspen Plus Radfrac block using the Peng–Robinson equation of state

er, respectively. Sharp enthalpy change on the reboiler side suggests that the feed is subcooled, and a pre-heater should be installed. The horizontal gap between the pinch point and the ordinate in Fig. 7, which is about 200 kW, indicates the possible reduction in heat duties by reducing the reflux ratio with the expense of increasing number of stages to achieve the specified separation. Obviously, the increase in the capital cost for a taller column should be traded-off with savings in utility costs. Figure 7 also shows that reboiler side is relatively close to ideal operation while the condenser side is far from ideal operation.

The total exergy of multicomponent streams are calculated from the three contributions: exergy change due to mixing, chemical exergy, and physical exergy. The exergy of mixing results from the isothermal and isobaric mixing of streams at actual process conditions. The chemical exergy is the difference in chemical potentials between the process components and the reference components in their environmental concentration, temperature, and pressure.

Energy saving in separation systems, particularly in distillation systems, is a research field that has attracted considerable innovative approaches. Distillation system is an essential separation process yet inefficient in using the thermal energy, and may operate with adverse environmental impact as it discharges a large amount of thermal energy into the environment. Innovative research incorporating the principles of thermodynamics for energy efficient distillation systems is in an advanced stage through pinch analysis, exergy analysis, and equipartition principle [25,116–120]. However, the thermodynamic analysis is still not widely used in design, retrofits, economic analysis of separation processes.

5.4 Equipartition Principle

The equipartition principle shows that the best trade-offs between entropy production and transfer area in transport processes are possible when the thermodynamic driving forces are uniform over the transfer area. For example, in a rate-controlled chemical reaction, the distribution of driving force $\Delta G/T$ should be uniform through space and time in the reactor system. The term ΔG is the change in the Gibbs energy for a reaction. For example, mathematical models show that uniform driving force across every stage yields a substantial decrease in energy consumption [18–20,25,127].

Some options for achieving a thermodynamic optimum are to improve an existing design so the operation will be less irreversible and distribute the irreversibilities uniformly over space and time. This approach relates the distribution of irreversibilities to the minimization of entropy production based on linear nonequilibrium thermodynamics. For a transport of single substance, the local rate of entropy production S_{prod} is

$$S_{\text{prod}} = JX \tag{5.18}$$

where J is the local flow of the substance and X is the conjugate driving force. Assuming that the linear phenomenological relations hold between the flow J and force X, we have

$$J = LX \tag{5.19}$$

where L is a phenomenological coefficient assumed constant and positive [25]. The total entropy production P is the integral of S_{prod} over the time t and space variables

$$P = \int\int S_{\text{prod}} \mathrm{d}V\,\mathrm{d}t = L\int\int X^2 \mathrm{d}V\,\mathrm{d}t \tag{5.20}$$

The total flow is the integral over time and space (volume V) of the local flow

$$J = L\int\int X \mathrm{d}V\,\mathrm{d}t = LVtX_{\text{av}} \tag{5.21}$$

where X_{av} is the average driving force. The total rate of entropy production from Eq. (5.20) is $P_{\text{av}} = JX_{\text{av}}$.The difference between the general case and the average value is [25]

$$\begin{aligned} P - P_{\text{av}} &= L\left[\int\int X^2 \mathrm{d}V\,\mathrm{d}t - (X_{\text{av}})^2 Vt\right] \\ &= LVt[(X^2)_{\text{av}} - (X_{\text{av}})^2] \end{aligned} \tag{5.22}$$

The square bracket on the right of Eq. (5.22) is the difference between the mean square and the square mean of the force distribution. Therefore, we have

$$\frac{P - P_{\text{av}}}{Vt} > 0 \text{ or } P_{\text{av}}\,(\text{equipartitioned}) < P\,(\text{arbitrary}) \tag{5.23}$$

The entropy production P_{av} of a process with a uniform driving force is smaller than that of a nonuniform situation with the same size, duration of the same average driving force, and the same overall load J. The local rate of entropy production S_{prod} will be uniform when the force X is uniform. Therefore, the equipartition of forces is analogous to equipartition of entropy production.

Consider the example of countercurrent and cocurrent heat exchangers shown in Fig. 8. Temperature profiles show that the driving force ΔT, or $1/\Delta T$, is more uniformly distributed in the countercurrent than in the cocurrent flow operation. This is the basic thermodynamic reason why a countercurrent is better than a cocurrent operation. The amount of heat transferred of the exchangers depends on the flow rate and inlet and outlet temperatures T_1 and T_2 of cold streams. The heat exchangers are identical except for the flow arrangements. The cocurrent exchanger will require a higher flow rate and/or higher temperature of hot fluid, and hence the operating cost

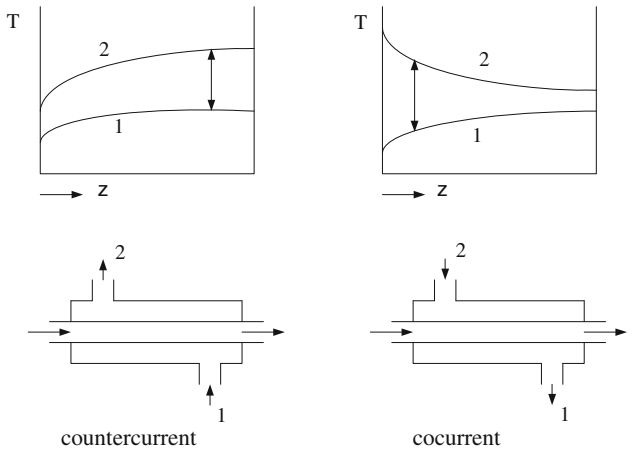

Fig. 8 Heat exchangers with countercurrent and cocurrent operations

will be higher than that of the countercurrent exchanger. Alternatively, the cocurrent exchanger will require a larger heat transfer area (greater initial investment) for a specified flow rate and inlet temperature of the hot fluid. Therefore, the countercurrent exchanger may minimize operating or investment costs compared with the cocurrent exchanger [127].

Case Study: Distillation Systems with Isoforce Operation

Adiabatic columns are highly irreversible and often the irreversibility is not evenly distributed. The stage-exergy loss profiles indicate the distribution of stage irreversibility and hence the distribution of driving forces in a column operation. Distillation columns operating with close to uniform thermodynamic forces are analyzed for separating n-pentane from n-heptane (Table 7), and ethanol from water (Table 8). These tables indicate clearly that a thermodynamically optimum distillation column should operate with close to uniform driving forces in separation. This is in line with the operation in which exergy loss is distributed evenly within the column. However, in minimizing the exergy loss or the rate of entropy production, one should avoid operation with too small driving forces (pinch in separation) at any stage.

The equipartition principle is mainly investigated for binary separations by distillation and should be extended

Table 7 Reboiler and condenser duties and entropy production change of an adiabatic distillation column with heat integration and isoforce for n-pentane and n-heptane mixture [122]

Operation	q_R (MW)	q_C (MW)	Reduction in entropy production (%)
Adiabatic	2.37	0.704	–
Isoforce	1.89	0.732	13.56
Near optimum	1.90	0.797	13.33

Table 8 Comparison of the performance of a diabatic column with a isoforce column operation for separation of ethanol–water mixture [19,20]

Operation	Total exergy losses (kJ/h)	Distillate flow rate (kg/h)	Distillate composition (%)
Adiabatic	44.23	0.969	87.53
Isoforce	14.24	0.974	87.13
Diabatic	15.89	0.973	87.22

to multicomponent separations with nonideal mixtures and by accounting the coupling between driving forces [19,20]. However, the general principle is not restricted to binary systems only. Still, the treatment of multicomponent diffusion as opposed to binary diffusion is fundamentally different. Multicomponent diffusion is much more appropriately treated by means of the Stefan-Maxwell equations, which involve setting up equations relating the corresponding thermodynamic forces to mass fluxes of all the components.

5.5 Gibbs Free Energy Minimization

For an ideal gas system, the total Gibbs energy is

$$G = \sum_i n_i G_i^o + \sum_i n_i RT \ln yi + \sum_i n_i RT \ln P \qquad (5.24)$$

where n_i is the number of moles of species i, G_i^o Gibbs energy of species i, at its standard state, G is the total Gibbs energy, y_i is the mole fraction of species i, R is the gas constant. If another state, such as liquid, exits then the Gibbs free energy for that state at the same T and P would be added on the right-hand side of Eq. (5.24). Thermodynamic analysis involves finding the compositions of species n_i at specified values of T and P, which minimizes of the total Gibbs energy subject to the constraints of elemental mass balance

$$m_k = \sum_i n_i \alpha_{ik} \qquad (5.25)$$

where α_{ik} is the number of atoms of the kth element in each molecule of species i, and m_k is the total number of atomic mass of the kth element in the system. Thermodynamic analysis based on temperature and the feed reactants ratio of fatty acid esterification for fatty acid alkyl esters production may be performed using the Gibbs free energy minimization for chemical and phase equilibrium calculations [128]. In another application, the equilibrium compositions under various operating conditions are estimated for the glycerol autothermal reforming to produce hydrogen for fuel cell application [91] by using the Gibbs free energy minimization.

Exergy analysis may be helpful for a bioethanol production process from lignocellulosic feedstock via a biochemical process to assess the overall thermodynamic efficiency

and identify the main loss processes [90]. The major inefficiencies of this process were identified as the combustion of lignin for process heat and power production and the simultaneous saccharification and co-fermentation processes [90]. With a Gibbs free energy minimization method, ethanol oxidative steam reforming can be carried out to estimate equilibrium state at various temperatures and pressures [92]. Thermodynamic analysis of the reforming of methane with carbon dioxide alone ("dry reforming") and with carbon dioxide and steam together ("mixed reforming") is performed to investigate the suitability of these endothermic reactions for the storage of solar thermal energy. The Gibbs free energy minimization method may identify thermodynamically optimal operating conditions for dry reforming as well as mixed reforming with a desired H_2/CO molar ratio of 2 [93].

Thermodynamic equilibrium calculations are estimated by minimizing Gibbs free energy to identify the operating conditions that maximize hydrogen production from a mixture of water and glycerol in thermo neutral condition [89]. Thermodynamic equilibrium of ethanol partial oxidation is studied by Gibbs free energy minimization method for hydrogen production at various operating conditions to find the maximum conversion of ethanol to hydrogen [92]. Thermodynamic equilibrium of methane autothermal reforming at various operating conditions [85] and aqueous phase reforming of methanol, acetic acid, and ethylene glycol for hydrogen production from bio-oil [86] are studied by Gibbs free energy optimization. Thermodynamic equilibrium analysis with is performed for stream reforming and autothermal steam reforming of vegetable oils to hydrogen and synthesis gas is investigated [87].

Using electrochemical and thermodynamic analyses, overall efficiency under different conditions may be calculated for high-temperature steam electrolysis of large-scale hydrogen production [88]. An ideal thermodynamic model of heat regeneration cycle in porous medium engine is developed to predict the thermodynamic performance [60]. Thermodynamic performance of the supercritical water reforming of glycerol for maximum power production is carried out by energy and exergy analyses [89].

If the reactions are not known in a chemical system, the Gibbs energy minimization at specified temperature and pressure can determine the equilibrium compositions of the system with single or multiple states.

5.6 Thermoeconomics

Thermoeconomics combines thermodynamic principles with economic analysis. Therefore, it may bring some fundamental changes in the economic evolution, design, and maintenance of processes. The exergy analysis cannot determine real design optima when monetary costs are brought into the picture. This has initiated an effort based on combined economics and thermodynamics field and is called as 'thermoeconomics', which developed to industrial standards in the past decade or so [1,2,4,9,11,23,38,102,103]. In this approach, efficiencies are calculated via an exergy analysis, and 'non-energy costs' (capital, interest, overhead, labor, maintenance, insurance, etc.) are related to the technical and thermodynamic parameters of the process under consideration. This exergy-aided cost optimization consists in determining the design point and the operative schedule that minimize the overall (monetary) cost, under a proper set of financial, normative, environmental, and technical constraints [2–12].

Thermoeconomics assigns costs to exergy-related variables using the exergy cost theory and exergy cost balances. This may lead to unifying mass, energy, exergy, and cost considerations by a single formulation. There are two main groups of thermoeconomic methods: (a) cost accounting methods and optimization methods, such as exergy cost theory for a rational price assessment, and (b) optimization by minimizing the overall cost, under a proper set of financial, environmental, and technical constraints, to identify the optimum design and operating conditions. Cost accounting methods use average costs as a basis for a rational price assessment, while optimization methods employ marginal costs in order to minimize the costs of the products of a system or a component. Environmental costs (in the monetary sense) can be included in thermoeconomic analyses by expanding the control volume beyond the plant under consideration to include immediate surroundings [6–8,21]. Process calculations must be then accordingly extended by assuming that the effluents from this enlarged control volume are at average conditions equal to those of the general environment [2,6,13,23].

Structural theory facilitates the evaluation of exergy cost and the incorporation of thermoeconomic functional analysis [11]. Structural theory is a common formulation for the various thermoeconomic methods. It provides costing equations from a set of modeling equations for the components or units of a system and display how the resource consumption is distributed among the components of a system. The flows entering a component in the productive structure are considered fuels F and flows leaving a component are products P. Therefore, the productive structure is a graphical representation of the fuel and product distribution. For any component j, or a subsystem, the unit exergy consumption ex_c on a fuel/product basis is

$$ex_{cj} = \frac{F_j}{P_j} = \frac{F_j}{\dot{E}x_j} \tag{5.26}$$

For linear modeling, the average costs of fuels and products are defined by

$$C^*_{jm} = \frac{\partial F_o}{\partial m_j}, \quad C^*_{jp} = \frac{\partial F_o}{\partial P_j} \tag{5.27}$$

where F_o is the fuel to the overall system expressed as a function of the flow m_j or product P_j, respectively, and the other related parameters. The total annual production cost C_T in \$/(kW h) is

$$C_T = \sum_{j=1}^{N} c_j \dot{E}x_j = \sum_{j=1}^{N} C_{jF} \tag{5.28}$$

where c_j is the product j in \$/(kW h), C_{jF} is the cost of fuel, and Ex_j is the rate of exergy as a product of component j in kW

5.7 Exergoeconomics

Exergoeconomics converts monetary expenses in to the equivalent exergy fluxes [2,4,9,21,23,129–131]. Optimization of an objective function for a process is based on these exergy fluxes [4,5]. Exergoeconomic analyses consider the quality of energy (exergy) in allocating the production costs of a process to the different products it produces. A general methodology for this kind of analysis was presented by Tsatsaronis in 1985 [4], which has later been called the exergoeconomic accounting technique [2,9]. Normally, in conducting an exergoeconomic balance, a system of simultaneous equations with a higher number of unknowns than equations is obtained, and thus some additional equations are required. Several approaches to solve this problem in cogeneration systems have been presented in [17], but in the case of crude oil refining processes the problem is much more complex due to the high number of simultaneous products [12].

5.8 Extended Exergy Analysis

An extended representation of exergy flow diagrams constitutes a substantial generalization of Szargut's cumulative exergy consumption procedure and may provide a coherent and consistent framework for including non-energetic quantities like capital cost, labor cost, and environmental impact into an engineering optimization procedure. In this sense, the environomic approach [21,119–136] represents already a significant extension of thermoeconomics, though its 'environmental penalty' functions suffer from their direct dependence on monetary cost. Some of the difficult issues that are to be addressed with a purely monetary or even with a thermoeconomic approach may be resolved in a straightforward manner by extended exergy accounting (EEA) [1,2]. As an indication of the potential of the method, various qualitative examples are offered of the application of EEA [1,6,7,15, 21,136]. More recently [6–9], an exergetic approach to the calculation of environmental costs has been proposed for establishing exergy as the only proper measure of environmental impact. EEA can be properly considered a further development of the pre-existing theories and methods of 'engineering cost analysis'.

Many suggest that the environmental impact of energy resource use and the achievement of increased efficiency may be best addressed by considering the thermodynamic property exergy. It is mainly concluded that thermodynamics, and particularly exergy, has a significant role to play in evaluating energy technologies and environmental impact. The results indicate that exergy methods should prove useful to engineers and scientists, as well as decision and policy makers. To increase the acceptance of exergy, further research is needed to better define its role in the area of environmental impact [6–8,13,16,21,26].

EEA may be capable of properly addressing environmental issues [6,8,136]. In an earlier work, a cumulative energetic index, later called 'embodied energy or 'emergy' for environmental accounting, was proposed [2]. Emergy is distant from the engineering concept of energy flow and of efficiency that its use as a design procedure is questioned. One of the goals of EEA is to proceed beyond thermoeconomics and to develop a formally complete costing theory based indifferently on an exergetic or on a monetary metric (that is, a general pricing method in which kJ/kg or kJ/kW are perfectly and consistently equivalent to /kg and /kW, respectively) [1,2,6,9].

A natural extension of life cycle assessment may be therefore the exergetic life-cycle analysis (ELCA) [1,2], which performs a lifelong analysis of a plant or process using exergy as a quantifier, thus expanding the capabilities of the 'energetic life cycle analysis'. ELCA includes items as labor, environmental damage, and recycle of energy and matter [1,2].

The attribute 'extended' refers to the additional inclusion in the exergetic balance of previously neglected terms, such as labor and to environmental remediation expenditures. The word 'accounting' has been independently suggested as a reminder that exergy does not satisfy a balance proper, in that the unavoidable irreversibilities of real processes irrevocably destroy a portion of the incoming exergy [5]. Extended exergetics is defined by its raw state exergy, augmented by the sum of all the net exergetics inputs received, directly or indirectly, in various processes pertaining to its extraction, preparation, transportation, and pre-treatment, including the exergetic equivalents of labor, capital, and environmental costs [2].

There is a possibility that some of the efforts might be overstating the consequences of the laws of thermodynamics [118] as it tries to combine the thermodynamic imperfections with the profitability of a product as well as the environmental and social issues.

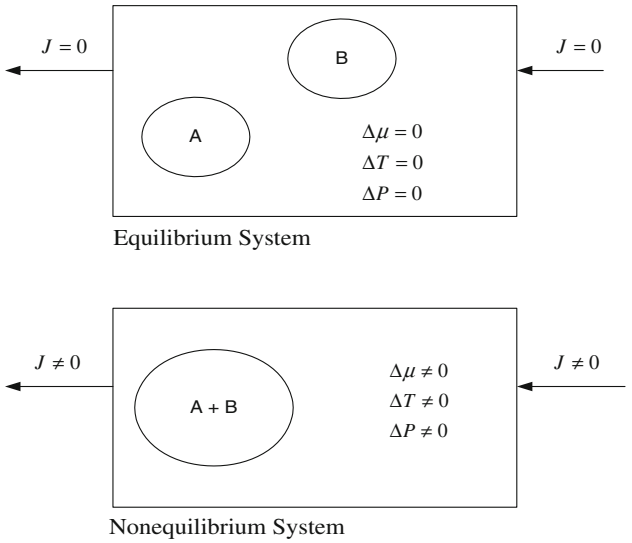

Fig. 9 Equilibrium and nonequilibrium systems

6 Nonequilibrium Thermodynamics

Natural systems consist of flows caused by unbalanced driving forces, and hence the description of such systems requires a larger number of properties in space and in time. Such systems are away from the global equilibrium state and are called *nonequilibrium systems* ; they can exchange energy and matter with the environment, and have finite driving forces (Fig. 9). The formalism of nonequilibrium thermodynamics can describe such systems in a qualitative and quantitative manner [25,28,29].

The first attempts to develop nonequilibrium thermodynamics theory occurred after the first observations of the coupled phenomena such as thermal diffusion and thermoelectric. Later, Onsager developed the basic equations of the theory, and Casimir, Meixner, and Prigogine refined and developed the theory further. States away from global equilibrium are called the thermodynamic branch (Fig. 10). When the distance from global equilibrium reaches a critical point, the states may become metastable or unstable. In this nonlinear region bifurcations and multiple solutions may occur. Regardless the distance from global equilibrium, the rate of entropy production is the product of independent flows and forces ($\dot{S}_{\text{prod}} = \sum_i J_i X_i$).

In its more general form, fluctuation theorems provide an analytical description of how irreversible macroscopic behavior evolves from time-reversible microscopic dynamics as either the system size or the observation time increases [27,28]. Therefore, fluctuation theorems bridge the microscopic and macroscopic domains, link the time-reversible and irreversible descriptions, help understanding the unique properties of microscopic and mesoscopic systems, and may serve as the basis for a theory of the nonequilibrium thermodynamics of small systems.

6.1 Linear Nonequilibrium Thermodynamics

The linear nonequilibrium thermodynamics theory determines the rate of entropy production to describe transport and rate processes in the vicinity of equilibrium, where phenomenological equations between independent flow flows J and forces X are linear ($J_i = L_{ik} X_k$) and the cross coefficients L_{ik} obey Onsger's reciprocal rules. The rate of entropy production equation identifies the independent forces and flows in various processes in a system. Linear flow–force relations are valid when the Gibbs free energy ranges less than 1.5 kJ/mol for chemical reactions. The formalism of linear nonequilibrium thermodynamics can be used in wider ranges (over a 7 kJ mol^{-1}) than usually expected with an error in the reaction velocity less than 15 % for some reactions. This theory is particularly useful to describe coupled

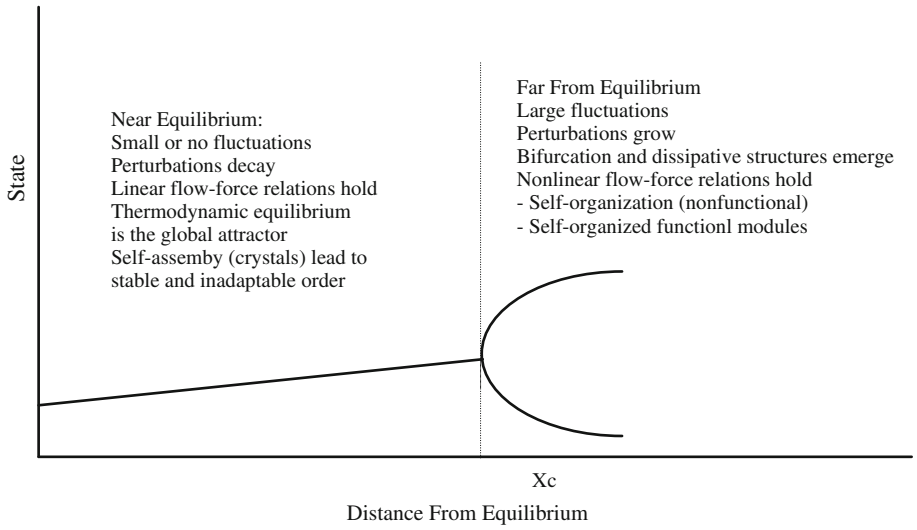

Fig. 10 Thermodynamic branch [25] showing the properties systems away from global equilibrium. Far from global equilibrium emerges after a critical distance characterized by critical thermodynamic force X_c

phenomena and quantify the level of coupling in transport and rate processes in physical, chemical, and biological systems without detailed process mechanisms [25]. The thermodynamic coupling refers that a flow occurs without or against its primary thermodynamic driving force, which may be a gradient of temperature, or chemical potential, or reaction affinity [28,29].

Reaction-transport systems represent open systems with thermodynamic forces of temperature gradient, concentration gradient, and affinity. Consider a reversible homogeneous elementary reaction between a substrate (S) and a product (P) $\mathrm{S} \underset{k_b}{\overset{k_f}{\rightleftarrows}} \mathrm{P}$. This type of reaction system is a common chemical system such as unimolecular isomerization. Using no volume flow condition ($\mathbf{J}_S V_S + \mathbf{J}_P V_P = 0$). The local rate of entropy production with the Gibbs–Duhem equation at constant temperature T and pressure $P(C_S \nabla \mu_S + C_P \nabla \mu_P = 0)$, is [25,34–37]:

$$\dot{S}_{\mathrm{prod}} = -\mathbf{J}_q \left(\frac{1}{T^2}\right) \nabla T - \mathbf{J}_S \frac{1}{T} \lambda_S \nabla C_S + J_{rS} \frac{A}{T} \geq 0, \quad (6.1)$$

where V_i is the partial molar volume of species i, and C_i is the concentration of species i.

$$\lambda_S = \left(1 + \frac{C_S}{C_P}\right) \left(\frac{\partial \mu_S}{\partial C_S}\right)_{T,P} \quad \text{for } (V_S \approx V_P)$$

The linear phenomenological equations show that all the forces contribute for each flow [34–37]:

$$\mathbf{J}_S = -D_{S,e} \nabla C_S - D_{T,e} \nabla T + \mathbf{L}_{Sr} \frac{A}{T}, \quad (6.2)$$

$$\mathbf{J}_q = -D_{D,e} \nabla C_S - k_e \nabla T + \mathbf{L}_{qr} \frac{A}{T}, \quad (6.3)$$

$$J_{\mathrm{r}} = -\mathbf{L}_{rS} \frac{1}{T} \lambda_S \nabla C_S - \mathbf{L}_{rq} \frac{1}{T^2} \nabla T + \frac{k_{\mathrm{f}} C_{S,eq}}{R} \frac{A}{T}, \quad (6.4)$$

where $D_{T,e}$ and $D_{D,e}$ are related to the thermal diffusion and the Dufour effect, respectively, and represent cross effects due to thermodynamic coupling, and k_e is the effective thermal conductivity [36,37]. Onsager's reciprocal relations states that $L_{ik} = L_{ki} (i \neq k)$ if J_i and J_k have the same parity under time reversal, and $L_{ik} = -L_{ki}$ if J_i and J_k have the opposite parity. In the absence of pertinent symmetries or invariances, all types of cross-couplings are possible. If the structure of the system is invariant with respect to some or all of the orthogonal transformations, then the invariance will eliminate certain cross-couplings and their cross-coefficients will vanish.

Equations (6.2) to (6.4) can be used in the well-known mass and energy balance equations

$$\frac{\partial C_S}{\partial t} = -\nabla \cdot \mathbf{J}_S + \nu_S J_{\mathrm{r}}, \quad (6.5)$$

$$\frac{\partial C_P}{\partial t} = -\nabla \cdot \mathbf{J}_P + \nu_P J_{\mathrm{r}}, \quad (6.6)$$

$$\rho c_p \frac{\partial T}{\partial t} = -\nabla \cdot \mathbf{J}_q + (-\Delta H_{\mathrm{r}}) J_{\mathrm{r}}, \quad (6.7)$$

where $\mathbf{J}_i$ is the vector of mass flows for species i, $\mathbf{J}_{\mathrm{q}}$ the vector of reduced heat flow $\mathbf{J}_q = \mathbf{q} - \sum_{i=1}^{n} \mathbf{J}_i H_i$, q is the total heat flow, H_i the partial molar enthalpy of species i, and ΔH_{r} the heat of reaction, C_i the concentration of species i, c_p the heat capacity, and ρ is the density. The reaction velocity is $\frac{\mathrm{d}C_S}{\nu_S \mathrm{d}t} = \frac{\mathrm{d}C_P}{\nu_P \mathrm{d}t} = J_{\mathrm{r}}$, and the parameters ν_S and ν_P are the stoichiometric coefficients, which are negative for reactants ($\nu_S = -1$). The modeling of thermodynamically and mathematically coupled system in one-dimensional form becomes [25,34–37]:

$$\frac{\partial \theta_S}{\partial \tau} = \frac{\partial^2 \theta_S}{\partial z^2} + \varepsilon \frac{\partial^2 \varphi}{\partial z^2} + \frac{\sigma}{\varphi^2} \frac{\partial \varphi}{\partial z} - A^* \mathrm{Da}_S \theta_{S,eq} \exp\left[\gamma_{\mathrm{f}} \left(1 - \frac{1}{\varphi}\right)\right], \quad (6.8)$$

$$\frac{1}{\mathrm{Le}} \frac{\partial \varphi}{\partial \tau} = \frac{\partial^2 \varphi}{\partial z^2} + \omega \frac{\partial^2 \theta_S}{\partial z^2} - \frac{\kappa}{\varphi} \frac{\partial \theta_S}{\partial z} + A^* \mathrm{Da}_S \beta \theta_{S,eq} \exp\left[\gamma_{\mathrm{f}} \left(1 - \frac{1}{\varphi}\right)\right], \quad (6.9)$$

$$\varepsilon = \frac{D_{T,e} T_s}{D_{S,e} C_{Ss}}, \omega = \frac{D_{D,e} c_s}{k_e T_s}, \sigma = \frac{[L_{rq} + L_{Sr}(-\Delta H_{\mathrm{r}})]L}{T_s D_{S,e} C_{Ss}},$$

$$\kappa = \frac{[L_{rq} + L_{Sr}(-\Delta H_{\mathrm{r}})] C_{Ss} L \lambda_S}{k_e T_s^2}$$

and

$$A^* = \left(\frac{\gamma_b - \gamma_{\mathrm{f}}}{\varphi}\right) + \ln\left(\frac{\theta_S}{K[a_1 + a_2(1-\theta_S)]}\right);$$

$$z = \frac{y}{L}, \tau = \frac{D_{S,e} t}{L^2}, \mathrm{Da}_S = \frac{L^2 k_o \exp(E_{\mathrm{f}}/RT_s)}{D_{S,e}},$$

$$\gamma_{\mathrm{f}} = \frac{E_{\mathrm{f}}}{RT_s}, \gamma_b = \frac{E_b}{RT_s}, \mathrm{Le} = \frac{k_e/\rho C_p}{D_{S,e}},$$

$$\theta_S = \frac{C_S}{C_{Ss}}, \theta_P = \frac{C_P}{K C_{Ss}}, a_1 = \frac{C_{Ps}}{K C_{Ss}}, a_2 = \frac{D_{S,e}}{K D_{P,e}},$$

$$\varphi = \frac{T}{T_s}, \beta = \frac{(-\Delta H_{\mathrm{r}}) D_{S,e} C_{Ss}}{(-\nu_S) k_e T_s},$$

The parameters ε, σ, ω, and κ are associated with the cross coefficients and hence control the induced flows because of the coupled reaction-transport system. Specifically, the ε and ω control the coupling between mass and heat flows, while the σ and κ control the coupling between the chemical reaction and mass flow, and chemical reaction and heat flow,

respectively. Therefore, induced effects due to various coupling phenomena can increase the possibility that the system may evolve to multiple states and diversify its behavior [25,28,29].

6.2 Extended Nonequilibrium Thermodynamics

When the distance from global equilibrium is beyond a critical point X_c, the states in the thermodynamic branch become metastable or unstable (Fig. 10). Prigogine called these states as dissipative structures, which may be highly organized and ordered states, and need a constant supply of mass and energy from the outside. Self-organized structures can emerge with an ability to reduce the effect of the applied gradients. For the systems far away from global equilibrium the relations between the general flows and forces are nonlinear [25]. In this region, chemical reactions and transport processes are characterized by the local potentials in which each macroscopic variable is described by an average quantity and fluctuating quantity. The compensation function and generalized hydrodynamics are an integral part of the extended theory of irreversible processes [25,137]. For understanding the highly nonlinear behavior of complex fluids and polymer mixtures, extended nonequilibrium thermodynamics may be very helpful [139,140]. Also the nonequilibrium thermodynamics may play important role to fully develop the theory of coarse graining for understanding through simplicity [139].

The thermal vibration phenomenon occurring in the dual-phase-lagging heat conduction violates the second law of thermodynamics under the local equilibrium assumption. The extended irreversible thermodynamics may help the dual-phase-lagging heat conduction model compatible with the second law of thermodynamics. It is also shown that these extended irreversible thermodynamics can give rise to the Maxwell model for the viscoelastic fluid flow [137,138].

6.2.1 Rarefied Gases

It is well known that the Navier–Stokes–Fourier equations as well as linear nonequilibrium thermodynamics cannot describe rarefaction effects in gases, which appear in processes with Knudsen numbers Kn > 0:05 [141–143]. A variety of extended models can be derived from the Boltzmann equation to describe rarefied gas flows at least approximately. The nonequilibrium thermodynamics of a multicomponent gas mixture may be formulated for the moment method and Burnett approximation and the boundary conditions including the slip and jump effects may be derived for slightly rarefied gases [143]. One of the applications is the transport processes in discontinuous systems and gas flows over solid bodies. The light scattering in extremely rarefied gases is studied within the extended thermodynamics, which is essentially a thermodynamic theory of irreversible processes in rarefied gases [139], involving symmetric hyperbolic field equations.

7 Statistical Thermodynamics

Statistical thermodynamics uses statistics of a large number of particles (probability theory) to relate the macroscopic properties to microscopic properties that are the molecular nature of the system [144,147]. Macroscopic properties include heat capacity, chemical and physical equilibrium constants, and equation of state. If n_i represents a distinct microstate of the system, the energy of this microstate is

$$E_i = \sum_{\substack{\text{all molecular}\\ \text{energy states j}}} n_{i,j}\varepsilon_j \tag{7.1}$$

where ε_j is the energy of the jth energy state of a single molecule. The probability of occurrence of a particular microstate i, p_i, with energy E_a is

$$p_i = \frac{e^{-E_a/k_BT}}{Q} \tag{7.2}$$

where k_B is the Boltzmann constant (1.3806×10^{-23} J/K) and Q is the partition function defined as

$$Q = \sum_{\text{states } i} e^{-E_i/k_BT} \tag{7.3}$$

Equation (7.2) shows that a state of higher energy has a lower probability of occurrence than a lower energy state. The Gibbs entropy equation can be written in terms of partition function and the probability of occurrence

$$\begin{aligned} S &= k_B\left(\ln Q + T\left(\frac{\partial \ln Q}{\partial T}\right)_{N,V}\right) \\ &= -k_B \sum_{\text{states } i} p(N,V,E_i)\ln p(N,V,E_i) \end{aligned} \tag{7.4}$$

where N is the number of particles and V is the volume. This definition is valid even when the system is far away from equilibrium, while other definitions assume that the system is in thermal equilibrium. The Gibbs entropy equation relates the entropy to probability of occurrence of the possible states of the system. If there are two equally probable states, then $p = 0.5$ and the entropy estimations yield

$$S = -k_B(0.5\ln(0.5)+0.5+\ln(0.5)] = -k_B\ln(0.5) = 0.693k_B$$

If there are 100 equally likely states, then

$$S = -k_B\ln(1/100) = 4.605k_B$$

As seen, if there are more equally probable states possible then the uncertainty as to which state the system occupy

increases and hence the entropy defined in terms of probability increases. Therefore, the statistical entropy is related to the uncertainty of knowledge about the state of the system and further is used as a measure of uncertainty contained in a communication that is imperfectly transmitted in the science of information.

Changes in the entropy by external effects are

$$\mathrm{d}S = -k_B \sum_{\text{states } i} \mathrm{d}p(N, V, E_i) \ln p(N, V, E_i) \tag{7.5}$$

The statistical thermodynamics methods may be used for computing standard free energy of noncovalent binding affinities. The derivation helps define clearly the changes in translational, rotational, configurational, and solvent entropy upon binding. 'Entropy and energy components of the binding free energy' analyzes the statistical-thermodynamic basis of energy component models for binding [147].

The material transport equations derived by nonequilibrium thermodynamics are used to describe the material transport in binary non-isothermal molecular systems. The chemical potentials of the components used in the equations are calculated using statistical mechanics. As the material transport equations contain chemical potentials at constant pressure, the local pressure distribution necessary in calculations is obtained using the condition of the local thermodynamic equilibrium around the selected molecular particle. The calculations yield the results equivalent to previous approaches and add new terms to the Soret coefficient, which are related to the difference in the translational and rotational thermal motion between the molecules. The proposed theory describes thermodiffusion in binary molecular systems with a limited miscibility. Nonequilibrium thermodynamic theory supplemented by microscopic calculations based on statistical mechanics allows for explaining most of the characteristic features of thermodiffusion in binary nonionic molecular mixtures [146]. Also, it relates mass and thermodiffusion properties to the critical temperature of the phase layering in the system with limited miscibility. Nonequilibrium statistical mechanics can connect the theory of macroscopic variables to atomic-level, Hamiltonian dynamics in phase space [148,149].

7.1 Equations of State

Equations of state describe the properties of fluids and mixtures of fluids for a set of specified physical condition. Kinetic theory and statistical thermodynamics are used for the prediction and correlation of physical and chemical properties of gases and liquids, including mixtures. For a gas composed of N identical particles, the configuration integral $Z(N, V, T)$ is based on the allowable kinetic and internal energy states

$$Z = \int_V \cdots \int_V \mathrm{e}^{-u(r_1 \ldots r_N)/k_B T} \mathrm{d}r_1 \ldots \mathrm{d}r_N \tag{7.6}$$

where spatial position of the particles is specified by the collection of N vectors $(r_1, r_2, \ldots r_N)$, and the potential energy interactions by $u(r_1, r_2, \ldots r_N)$. An expression for the interaction energy between the particles is needed to evaluate the configuration integral. When the configuration integral is known, all the thermodynamic properties of the system can be evaluated. For example, the ideal gas law is obtained when there is no energy interactions between the particles and all the nonideal effects in the equation of state are contained in the configuration integral. Some of the early examples are the virial equation of state and the derivation of Van der Waals equation of state by the statistical thermodynamics with particles interacting with each other. Some powerful and focused, such as for petroleum applications and supercritical fluids, equations of state derivations using the statistical thermodynamics are possible [144–151].

8 Thermodynamics and Sustainability

Sustainable development' has been defined as 'development that meets the needs of the present without compromising the ability of future generations to meet their own needs'. Adequate and affordable energy supplies have been the key to economic development and the transition from subsistence agricultural economies to modern industrial and service-oriented societies. Energy is central to improved social and economic well-being and is indispensable to most industrial and commercial wealth generation. When choosing energy fuels and associated technologies for the production, delivery, and use of energy services, it may be essential to take into account economic, social, and environmental consequences [6–8,13,16,26,136].

Muller [152–154] stated that randomization and a deterministic trend toward preferred states may be observed in other fields including sociology and economics that are remote from thermodynamics and proposed extrapolations of thermodynamics to such remote areas. Since exergy is a measure of the departure of the state of the system from that of the environment, it relates the system to the environment. When a system is in thermal, mechanical, and chemical equilibrium with the environment, there are no processes taking place in the environment.

Many factors including harnessing sustainable energy sources, utilizing sustainable energy carriers, increasing efficiency, reducing environmental impact, and improving socioeconomic acceptability may lead towards energy sustainability. The latter factor includes community involvement and social acceptability, economic affordability and equity, and lifestyles. Energy sustainability is of great importance to overall sustainability because of its importance in economic

development and living standards as well as its impact on the environment [6–8,21].

Thermodynamics and particularly exergy may have a significant role to play in evaluating the impact of energy technology on the environment. This may need to increase the acceptance of exergy by further research on the definition of the role of exergy clearly in the area of environmental impact [13]. For example, the environmental impact of emissions may be reduced by increasing the efficiency of resource utilization. Although increasing efficiency generally requires greater use of materials, labor, and advanced technologies, the additional cost may be justified by the resulting benefits. For exergy analysis, the characteristics of the reference environment must be specified for improving the efficiency of an energy source, for it quantifies the locations, types, and magnitudes of wastes and losses. The common approach in doing so is specifying the temperature, pressure, and chemical composition. Increasing efficiency also has sustainability implications as it makes the resources available for a longer time [6,7,13]. The three relationships between exergy and environmental impact are the loss of order, resource degradation, and waste exergy emissions. The loss of order is a form of environmental damage and the exergy of an ordered system is greater. The degradation of resources found in nature may be a form of environmental damage. Exergy associated with waste emissions can be a potential for environmental damage as it can cause change. However, the relationships between thermodynamic losses and capital costs for devices and processes need some clear examples and applications [6,11,13,21,133]. Many of the side effects of energy production and consumption may lead to resource uncertainties and potential environmental hazards on a local, regional, and global scale. Examples include

- the depletion of oil and natural gas resources,
- the generation of smog from urban road transport,
- the formation of acid rain via pollutant emissions from fossil fuel power stations,
- the difficulty of long-term safe storage of radioactive wastes from nuclear power plants,
- the possibility of the enhanced greenhouse effect from combustion-generated pollutants.

Consequently, the energy sector plays a pivotal role in attempts to achieve sustainable development: balancing economic and social development with environmental protection. Here, thermodynamic limits are represented as underpinning the environmental sphere. Sustainability may be a key concept for our future and the role of thermodynamics in its assessment may be fundamental. The use of energy and matter must be considered not only from a microscopic viewpoint (the use of a single fuel or material, or the presence of a single pollutant) but also by means of holistic approaches able to synthesize all the characteristics of a single process. Exergy may be a suitable function for this purpose. The exergy concept can also be applied to natural systems and to systems at the interface between natural and artificial ones [7,131–136].

9 Conclusions

In this review, thermodynamic analyses have been summarized under the following methodologies: (i) second law analysis, (ii) exergy analysis, (iii) pinch analysis, (iv) equipartition principle, (v) Gibbs free energy minimization, (vi) thermoeconomics, (vii) exergoeconomics, and (viii) extended exergy analysis. The exergy analysis, which is the most popular methodology, is discussed for the following systems: (1) power cycle applications, (2) biomass and coal gasification, (3) solar energy applications, (4) refrigeration, (5) waste heat utilization, (6) distillation column systems, and (7) heat and fluid flow in microchannels fluid flow systems. Thermodynamic analysis mainly is concerned with the following design questions: What is the total rate of entropy production? How is the entropy production distributed through the system?, How to design a system to minimize the rate of entropy production. More and more studies are addressing all the design questions above mainly for heat and fluid flow systems regardless of the level of energy intensity involved. Thermodynamic analysis may be more useful and effective if it keeps successfully expanding toward diverse and multiscale processes in physical, chemical, and biological systems. Besides that understanding and modeling complex and nonequilibrium systems in various scales by nonequilibrium and statistical thermodynamics are attracting scientist from diverse backgrounds. This trend may be a natural result of unifying power of thermodynamics in understanding time phenomena.

Thermoeconomics and exergoeconomics, and extended exergy accounting concepts tied the thermodynamic analysis, particularly the exergy analysis, to economics, environment, and eventually sustainability, which has three overlapping elements of economy, environment and society. However, the linking of methods of energy and exergy analyses to the pollutant emissions, socioeconomics, and engineering economics may be only indirect, and hence may provide an insufficient basis for environmental appraisal and for evaluating measures of sustainability in and beyond the energy sector.

References

1. Sciubba, E.: Extended exergy accounting applied to energy recovery from waste: the concept of total recycling. Energy **28**, 1315–1334 (2003)

2. Sciubba, E.: Exergo-economics: thermodynamic foundation for a more rational resource use. Int. J. Energy Res. **29**, 613–636 (2005)
3. Szargut, J.; Morris, D.R.; Steward, F.R.: Exergy Analysis of Thermal, Chemical and Metallurgical Processes. Hemisphere Publishing Corporation, New York (1988)
4. Tsatsaronis, G.; Winhold, M.: Exergoeconomic analysis and evaluation of energy-conversion plants. 1. A new general methodology. Energy **10**, 69–80 (1985)
5. Tsatsaronis, G.; Park, M.-Ho.: On avoidable and unavoidable exergy destructions and investment costs in thermal systems. Energy Convers. Manage. **43**, 1259–1270 (2002)
6. Dinçer, I.; Rosen, M.A.: Exergy: Energy, Environment, and Sustainable Development. Elsevier, Oxford (2007)
7. Dinçer, I.; Zamfirescu, C.: Sustainable Energy Systems and Applications, Springer, Oxford (2011)
8. Dinçer, I.; Midilli, A.; Hepbasli, A.; Karakoc, T.H. (eds.): Global Warming: Engineering Solutions. Springer, Oxford (2009)
9. Tsatsaronis, G.: Recent developments in exergy analysis and exergoeconomics. Int. J. Exergy **5**, 489–499 (2008)
10. Bejan, A.; Tsatsaronis, G.; Moran, M.: Thermal Design & Optimization. Wiley, New York (1996)
11. Valero, A.; Serra, L.; Uche, J.: Fundamentals of exergy cost accounting and thermoeconomics. Part II: applications. J. Energy Resour. Technol. **128**, 9–15 (2006)
12. Rivero, R.; Rendon, C.; Gallegos, S.: Exergy and exergoeconomic analysis of a crude oil combined distillation unit. Energy **29**, 1909–1927 (2004)
13. Rosen, M.A.: Assessing energy technologies and environmental impacts with the principles of thermodynamics. Appl. Energy **72**, 427–441 (2002)
14. Wall, G.: Conditions and tools in the design of energy conversion and management systems of a sustainable society. Energy Convers. Manage. **43**, 1235–1248 (2002)
15. Morosuk, T.; Tsatsaronis, G.: Advanced exergy analysis for chemically reacting systems-application to a simple open gas-turbine system. Int. J. Thermodyn. **12**, 105–111 (2009)
16. Rosen, M.A.: Energy sustainability: a pragmatic approach and illustrations. Sustainability **1**, 55–80 (2009)
17. Rivero, R.: Application of the exergy concept in the petroleum refining and petrochemical industry. Energy Convers. Manage. **43**, 1199 (2002)
18. Rivero, R.: Exergy simulation and optimization of adiabatic and diabatic binary distillation. Energy **26**, 561 (2001)
19. De Koeijer, G.M.; Kjelstrup, S.; Salamon, P.; Siragusa, G.; Schaller, M.; Offmann, K.H.: Comparison of entropy production rate minimization methods for binary diabatic distillation. Ind. Eng. Chem. Res. **41**, 5826 (2003)
20. De Koijer, G.; Rivero, R.: Entropy production and exergy loss in experimental distillation columns. Chem. Eng. Sci. **58**, 1587 (2003)
21. Ayres, R.U.: Eco-thermodynamics: economics and the second law. Ecol. Econ. **26**, 180 (1998)
22. Kelly, S.; Tsatsaronis, G.; Morosuk, T.: Advanced exergetic analysis: approaches for splitting the exergy destruction into endogenous and exogenous parts. Energy **34**, 384–391 (2009)
23. Petrakopoulou, F.; Tsatsaronis, G.; Morosuk, T.; Carassai, A.: Advanced exergoeconomic analysis applied to a complex energy conversion system. J. Eng. Gas Turbines Power **134**, 031801-8 (2012)
24. Morosuk, T.; Tsatsaronis, G.: A new approach to the exergy analysis of absorption refrigeration machines. Energy **33**, 890–907 (2008)
25. Demirel, Y.: Nonequilibrium Thermodynamics: Transport and Rate Processes in Physical, Chemical and Biological Systems, 2nd edn. Elsevier, Amsterdam (2007)
26. Hammond, G.P.: Engineering sustainability: thermodynamics, energy systems, and the environment. Int. J. Energy Res. **28**, 613–639 (2004)
27. Bejan, A.: Entropy Generation Minimization, 2nd edn. Elsevier, New York (1996)
28. Demirel, Y.; Sandler, S.I.: Nonequilibrium thermodynamics in engineering and science. J. Phys. Chem. B **108**, 31–43 (2004)
29. Demirel, Y.; Sandler, S.I.: Linear-nonequilibrium thermodynamics theory for coupled heat and mass transport. Int. J. Heat Mass Transfer **44**, 2439–2451 (2001)
30. Tzou, D.Y.: Macro- to Microscale Heat Transfer: The Lagging Behavior, Taylor & Francis, Washington (1997)
31. Tzou, D.Y.: Experimental support for the lagging response in heat propagation. AIAA J. Thermophys. Heat Transfer **9**, 686–693 (1995)
32. Zhou, J.; Chen, K.K.; Zhang, Y.: Dual-phase lag effects on thermal damage to biological tissues caused by laser irradiation. Comput. Biol. Med. **39**, 286–293 (2009)
33. Al-Nimr, M.A.; Naji, M.; Arpaci, V.: Non-equilibrium entropy production under the effect of dual-phase lag heat conduction model. ASME J. Heat Transfer **122**, 217–223 (2000)
34. Demirel, Y.: Thermodynamically coupled heat and mass flows in a reaction-transport system with external resistances. Int. J Heat Mass Transfer **52**, 2018–2025 (2009)
35. Demirel, Y.: Thermodynamically coupled transport in simple catalytic reactions. Int. J. Chem. Reactor Eng. **6**, 1–22 (2008)
36. Demirel, Y.: Modeling of thermodynamically coupled reaction-transport systems. Chem. Eng. J. **139**, 106–117 (2008)
37. Demirel, Y.: Non-isothermal reaction diffusion systems with thermodynamically coupled heat and mass transfer. Chem. Eng. Sci. **61**, 3379–3385 (2006)
38. Moran, M.J.; Shapiro, H.N.: Fundamentals of Engineering Thermodynamics, 4th edn. Wiley, New York (2000)
39. Demirel, Y.; Kahraman, R.: Entropy generation in a rectangular packed duct with wall heat flux. Int. J. Heat Mass Transfer **42**, 2337–2344 (1999)
40. Demirel, Y.; Al-Ali, H.H.: Thermodynamic analysis of convective heat transfer in a packed duct with asymmetrical wall temperatures. Int. J. Heat Mass Transfer **40**, 1145–1153 (1997)
41. Demirel, Y.; Al-Ali, H.H.; Abu-Al-Saud, B.A.: Entropy generation of convection heat transfer in an asymmetrically heated packed duct. Int. Commun. Heat Mass Transfer **24**, 381–390 (1997)
42. Sahin, A.Z.; Ayar, T.; Yilbas, B.S.: First and second law analyses of laser cutting process in relation to the end product quality. Int. J. Energy Res. **32**, 689–697 (2008)
43. Yilbas, B.S.; Bin Mansoor, S.: Entropy generation in laser heating in relation to machining. Heat Mass Transfer **44**, 331–341 (2008)
44. Sahin, A.Z.: Entropy generation in turbulent liquid flow through a smooth duct subjected to constant wall temperature. Int. J. Heat Mass Transfer **43**, 1469–1478 (2000)
45. Yilbas, B.S.; Sahin, A.Z.; Chatwin, C.; et al.: Laser cutting of Kevlar laminates: first and second law analysis. J. Mech. Sci. Technol. **25**, 855–862 (2011)
46. Alquaity, A.B.S.; Al-Dini, S.A.; Yilbas, B.S.: Entropy generation rate in microchannel flow with phase change particles. J. Thermophys. Heat Transfer **26**, 134–140 (2012)
47. Bilgen, S.; Kaygusuz, K.: Second law (exergy) analysis of cogeneration system. Energy Sources Part A **30**, 1267–1280 (2008)
48. Naterer, G.F.; Camberos, J.A.: Entropy Based Design and Analysis of Fluids Engineering Systems. CRC Press, New York (2008)
49. Demirel, Y.: Irreversibility profiles in a circular Couette flow of temperature dependent materials. Int. Commun. Heat Mass Transfer **26**, 75–83 (1999)

50. Demirel, Y.Y.: Thermodynamic analysis of thermomechanical coupling in Couette flow. Int. J. Heat Mass Transfer **43**, 4205–4212 (2000)
51. Demirel, Y.: Irreversibility Distribution for a pure convection case of the Smith-Hutton problem. Int. Commun. Heat Mass Transfer **25**, 671–679 (1998)
52. Demirel, Y.; Kahraman, R.: Thermodynamic analysis of convective heat transfer in an annular packed bed. Int. J. Heat Fluid Flow **21**, 442–448 (2000)
53. Demirel, Y.: Thermodynamic optimization of convective heat transfer in a packed duct. Energy **20**, 959–967 (1995)
54. Godoy, E.; Benz, S.J.; Scenna, N.J.: A strategy for economic optimization of combined cycle gas turbine power plants by taking advantage of useful thermodynamic relationships. Appl. Thermal Eng. **31**, 852–871 (2011)
55. Srinivas, T.; Gupta, A.V.S.S.K.S.; Reddy, B.V.: Generalized thermodynamic analysis of steam power cycles with 'n' number of feedwater heaters. Int. J. Thermodyn. **10**, 177–185 (2007)
56. Gao, L.; Jin, H.; Liu, Z.; Zheng, D.: Exergy analysis of coal-based polygeneration system for power and chemical production. Energy **29**, 2359–2371 (2004)
57. Eskin, N.; Gungor, A.; Ozdemir, K.: Thermodynamic analysis of a FBCC steam power plant. Energy Convers. Manage. **50**, 2428–2438 (2009)
58. Dincer, I.; Al-Muslim, H.: Thermodynamic analysis of reheat cycle steam power plants. Int. J. Energy Res. **25**, 727–739 (2001)
59. Abu-Nada, E.; Al-Hinti, I.; Akash, B.; Al-Sarki, A.: Thermodynamic analysis of spark-ignition engine using a gas mixture model for the working fluid. Int. J. Energy Res. **31**, 1031–1046 (2007)
60. Shyani, B.G.; Caton, J.A.: A thermodynamic analysis of the use of exhaust gas recirculation in spark ignition engines including the second law of thermodynamics. Proc. IMechE Part D: J. Automobile Eng. **223**, 131–149 (2009)
61. Liu, H.; Xie, M.; Wu, D.: Thermodynamic analysis of the heat regenerative cycle in porous medium engine. Energy Convers. Manage. **50**, 297–303 (2009)
62. Mitrovic, D.; Zivkovic, D.; Lakovic, M.S.: Energy and exergy analysis of a 348.5 MW steam power plant. Energy Sources **32**, 1016–1027 (2010)
63. Ozturk, H.K.; Atalay, O.; Yilanci, A.: Energy and exergy analysis of Kizildere geothermal power plant, Turkey. Energy Sources A **28**, 1415–1424 (2006)
64. Cihan, A.; Hacıhafızoglu, O.; Kahveci, K.: Energy–exergy analysis and modernization suggestions for a combined-cycle power plant. Int. J. Energy Res. **30**, 115–126 (2006)
65. Sanjay, Y.; Singh, O.; Prasad, B.N.: Energy and exergy analysis of steam cooled reheat gas-steam combined cycle. Appl. Thermal Eng. **27**, 2779–2790 (2007)
66. Sengupta, S.; Datta, A.; Duttagupta, S.: Exergy analysis of a coal-based 210 MW thermal power plant. Int. J. Energy Res. **31**, 14–28 (2007)
67. Khaliq, A.: Exergy analysis of gas turbine trigeneration system for combined production of power heat and refrigeration. Int. J. Refrigeration **32**, 534–545 (2009)
68. Cziesla, F.; Tsatsaronis, G.; Gao, Z.: Avoidable thermodynamic inefficiencies and costs in an externally fired combined cycle power plant. Energy **31**, 1472–1489 (2006)
69. Ehsan, A.; Yilmazoglu, M.Z.: Design and exergy analysis of a thermal power plant using different types of Turkish lignite. Int. J. Thermodyn. **14**, 125–133 (2011)
70. Sanjay, Y.; Singh, O.; Prasad, B.N.: Energy and exergy analysis of steam cooled reheat gas-stem combined cycle. Appl. Thermal Eng. **27**, 2779–2790 (2007)
71. Cihan, A.; Hacihafizoglu, O.; Kahveci, K.: Energy-exergy analysis and modernization suggestions for a combined-cycle power plant. Int. J. Energy Res. **30**, 115–126 (2006)
72. Sengupta, S.; Datta, A.; Duttagupta, S.: Exergy analysis of a coal-based 210 MW thermal power plant. Int. J. Energy Res. **31**, 14–28 (2007)
73. Khaliq, A.; Choudhary, K.; Dincer, I.: Exergy analysis of a gas turbine trigeneration system using the Brayton refrigeration cycle for inlet air cooling. Proc. IMechE 224 Part A. J. Power Energy **224**, 449–461 (2010)
74. Granovskii, M.; Dincer, I.; Rosen, M.A.: Exergy analysis of a gas turbine cycle with steam generation for methane conversion within solid oxide fuel cells. J. Fuel Cell Sci. Technol. **5**, 031005-1-9 (2008)
75. Duan, L.; He, B.; Yang, Y.: Parameter optimization study on SOFC-MGT hybrid power system. Int. J. Energy Res. **35**, 721–732 (2011)
76. Huang, Y.-C.; Hung, B.-I.; Chen, C.-K.: An ecological exergy analysis for an irreversible Brayton engine with an external heat source. Proc. Inst. Mech. Eng. **214**, 413–421 (2000)
77. Reddy, V.S.; Kaushik, S.C.; Tyagi, S.K.; Panwar, N.L.: An approach to analyze energy and exergy analysis of thermal power plants: a review. Smart Grid Renew. Energy **1**, 143–152 (2010)
78. Toonssen, R.; Woudstra, N.; Verkooijen, A.H.M.: Exergy analysis of hydrogen production plants based on biomass gasification. Int. J. Hydrogen Energy **33**, 4074–4082 (2008)
79. Bang-Moller, C.; Rokni, M.; Elmegaard, B.: Exergy analysis and optimization of a biomass gasification, solid oxide fuel cell and micro gas turbine hybrid system. Energy **36**, 4740–4752 (2011)
80. Shudo, Y.; Ohkubo, T.; Hideshima, Y.; Akiyama, T.: Exergy analysis of the demonstration plant for co-production of hydrogen and benzene from biogas. Int. J. Hydrogen Energy **34**, 4500–4508 (2009)
81. Kempegowda, R.; Assabumrungrat, S.; Laosiripojana, N.: Thermodynamic analysis for gasification of Thailand rice husk with air, steam, and mixed air/steam for hydrogen-rich gas production. Int. J. Chem. React. Eng. **8**, A158 (2010)
82. De, S.; Biswal, S.K.: Thermodynamic analysis of a coal gasification and split Rankine combined cogeneration plant. Part 2: energy analysis. Proc. IMechE **219**, 169–178 (2005)
83. De, S.; Biswal, S.K.: Thermodynamic analysis of a coal gasification and split Rankine combined cogeneration plant. Part 2: exergy analysis. Proc. IMechE **219**, 179–185 (2005)
84. Giuffrida, A.; Romano, M.C.; Lozza, G.: Thermodynamic analysis of air-blown gasification for IGCC applications. Appl. Energy **88**, 3949–3958 (2011)
85. Li, Y.; Wang, Y.; Zhang, X.; Mi, Z.: Thermodynamic analysis of autothermal steam and CO_2 reforming of methane. Int. J. Hydrogen Energy **33**, 2507–2514 (2008)
86. Xie, J.; Su, D.; Yin, X.; Wu, C.; Zhu, J.: Thermodynamic analysis of aqueous phase reforming of three model compounds in bio-oil for hydrogen production. Int. J. Hydrogen Energy **36**, 15561–15572 (2011)
87. Yenumala, S.R.; Maity, S.K.: Reforming of vegetable oil for production of hydrogen: a thermodynamic analysis. Int. J. Hydrogen Energy **36**, 11666–11675 (2011)
88. Mingyi, L.; Bo, Y.; Jingming, X.; Jing, C.: Thermodynamic analysis of the efficiency of high-temperature steam electrolysis system for hydrogen production. J. Power Sour. **177**, 493–499 (2008)
89. Ortiz, F.J.G.; Ollero, P.; Serrera, A.; Galera, S.: An exergy and exergy analysis of the supercritical water reforming of glycerol for power production. Int. J. Hydrogen Energy **37**, 209–226 (2012)
90. Sohel, M.I.; Jack, M.W.: Thermodynamic analysis of lignocellulosic biofuel production via a biochemical process: guiding technology selection and research focus. Bioresource Technol. **102**, 2617–2622 (2011)
91. Wang, H.; Wang, X.; Li, M.; Li, S.; Wang, S.; Ma, X.: Thermodynamic analysis of hydrogen production from glycerol autothermal reforming. Int. J. Hydrogen Energy **34**, 5683–5690 (2009)

92. Liu, S.; Zhang, K.; Fang, L.; Li, Y.: Thermodynamic analysis of hydrogen production from oxidative steam reforming of ethanol. Energy Fuels **22**, 1365–1370 (2008)
93. Sun, Y.; Ritchie1, T.; Hla, S.S.; McEvoy, S.; Stein, W.; Edwards, J.H.: Thermodynamic analysis of mixed and dry reforming of methane for solar thermal applications. J. Nat. Gas Chem. **20**, 568–576 (2011)
94. Caliskan, H.; Hepbasli, A.; Dincer, I.: Exergy analysis and sustainability assessment of a solar-ground based heat pump with thermal energy storage. J. Solar Energy Eng. ASME **133**, 011005-1-7 (2011)
95. Xiaowu, W.; Ben, H.: Exergy analysis of domestic-scale solar water heaters. Renewable Sust. Energy Rev. **9**, 638–645 (2005)
96. Jegadheeswaran, S.; Pohekar, S.D.: Exergy analysis of particle dispersed latent heat thermal storage system for solar water heaters. J. Renew. Sustain. Energy **2**, 023105-1-17 (2010)
97. Li, X.; Zhang, X.: Component exergy analysis of solar powered transcritical CO_2 Rankine cycle system. J. Thermal Sci. **20**, 195–200 (2011)
98. Nayak, S.; Tiwari, G.N.: Theoretical performance assessment of an integrated photovoltaic and earth air heat exchanger greenhouse using energy and exergy analysis methods. Energy Build. **41**, 888–896 (2009)
99. Hepbasli, A.; Utlu, Z.: Analyzing the energy utilization efficiency of renewable energy resources. Part 2: exergy analysis method. Energy Sources B **1**, 355–366 (2006)
100. Baghernejad, A.; Yaghoubi, M.: Exergy analysis of an integrated solar combined cycle system. Renew. Energy **35**, 2157–2164 (2010)
101. Ozturk, H.H.; Demirel, Y.: Exergy-based performance analysis of packed bed solar air heaters. Int. J. Energy Res. **28**, 423–432 (2004)
102. Demirel, Y.; Ozturk, H.H.: Thermoeconomics of seasonal heat storage system. Int. J. Energy Res. **30**, 1001–1012 (2006)
103. Demirel, Y.: Heat storage by phase changing materials and thermoeconomics. In: Paksoy, H.O. (ed.) Thermal Energy Storage for Sustainable Energy Consumption, pp. 133–151. Springer, London (2007)
104. Bascetincelik, A.; Ozturk, H.H.; Paksoy, H.O.; Demirel, Y.: Energetic and exergetic efficiency of latent heat storage system for greenhouse heating. Renew. Energy **16**, 691–694 (1999)
105. Nayak, S.; Tiwari, G.N.: Energy and exergy analysis of photovoltaic/thermal integrated with a solar Greenhouse. Energy Build. **40**, 2015–2021 (2008)
106. Xu, C.; Wang, Z.; Li, X.; Sun, F.: Energy and exergy analysis of solar tower plants. Appl. Energy **31**, 3904–3913 (2011)
107. Torío, H.; Schmidt, D.: Development of system concepts for improving the performance of a waste heat district heating network with exergy analysis. Energy Build. **42**, 1601–1609 (2010)
108. Terlizzese, T.; Zanchini, E.: Economic and exergy analysis of alternative plants for a zero carbon building complex. Energy Build. **43**, 787–795 (2011)
109. Ozgener, L.; Hepbasli, A.; Dincer, I.: Energy and exergy analysis of Salihli geothermal district heating system in Manisa, Turkey. Int. J. Energy Res. **29**, 393–408 (2005)
110. Ozgener, L.; Hepbasli, A.; Dincer, I.: Thermo-mechanical exergy analysis of Balcova geothermal district heating system in Izmir, Turkey. Int. J. Energy Res. **126**, 293–301 (2004)
111. Keçebas, A.; Kayfeci, M.; Gedik, E.; Performance investigation of the Afyon geothermal district heating system for building applications: exergy analysis. Appl. Thermal Eng. **31**, 1229–1237 (2011)
112. Yong, P.S.; Moon, H.M.; Yi, S.C.: Exergy analysis of cryogenic air separation process for generating nitrogen. J. Ind. Eng. Chem. **8**, 499 (2002)
113. Talbi, M.M.; Agnew, B.: Exergy analysis: an absorption refrigerator using lithium bromide and water as the working fluids. Appl. Thermal Eng. **20**, 619–630 (2000)
114. Dincer, I.: Refrigeration Systems and Applications, Wiley, New York (2003)
115. Parekh, A.D.; Tailor, P.R.: Thermodynamic analysis of R507A-R23 cascade refrigeration system. Int. J. Aerospace Mech. Eng. **6**, 35–39 (2012)
116. Maia, M.L.O.; Zemp, R.J.: Thermodynamic analysis of multicomponent distillation column: Identifying optimal feed conditions. Braz. J. Chem. Eng. **17**, 751 (2000)
117. Chang, H.S.; Chuang, S.C.: The intrinsic and extrinsic exergy losses of distillation columns. J. Chinese Inst. Chem. Eng. **32**, 469 (2001)
118. Bandyopadhyay, S.: Effect of feed on optimal thermodynamic performance of a distillation column. Chem. Eng. J. **88**, 175 (2002)
119. Al-Muslim, H.; Dincer, I.; Zubair, S.M.: Exergy analysis of single-and two-stage crude oil distillation units. J. Energy Resour. Technol. **125**, 199 (2003)
120. Demirel, Y.: Assessment of Thermodynamic performances for distillation columns. Int. J. Exergy **3**, 345–361 (2006)
121. Demirel, Y.: Retrofit of distillation columns by thermodynamic analysis. Separation Sci. Technol. **41**, 791–817 (2006)
122. Demirel, Y.: Thermodynamic analysis of separation systems. Separation Sci. Technol. **39**, 3897–3942 (2004)
123. Nguyen, N.; Demirel, Y.: Retrofit of distillation columns in biodiesel production plants. Energy **35**, 1625–1632 (2010)
124. Yarin, L.P.; Mosyak, A.: Gad Hetsroni, Fluid Flow, Heat Transfer and Boiling in Micro-Channels. Springer, Berlin (2009)
125. Kandlikar, S.G.; Garimella, S.; Li, D.; Colin, S.; King, M R.: Heat Transfer and Fluid Flow in Minichannels and Microchannels. Elsevier, Amsterdam (2006)
126. Dhole, V.R.; Linnhoff, B.: Overall design of low temperature processes. Comput. Chem. Eng. **13**, S105 (1994)
127. Tondeur, D.; Kvaalen, E.: Equipartition of entropy production. An optimality criterion for transfer and separation processes. Ind. Eng. Chem. Res. **26**, 50 (1987)
128. Voll, F.A.P.; da Silva, C.; Rossi, C.C.R.S.; Guirardello, R.; de Castilhos, F.; Olivera, J.V.; Cardozo-Filho, L.: Thermodynamic analysis of fatty acid esterification for fatty acid alkyl esters production. Biomass Bioenergy **35**, 781–788 (2011)
129. Zhang, G.; Hua, B.; Chen, Q.: Exergoeconomic methodology for analysis and optimization of process systems. Comput. Chem. Eng. **24**, 613 (2000)
130. Chen, Q.L.; Yin, Q.H.; Hua, B.: An exergoeconomic approach for retrofit of fractionating. Energy **27**, 65 (2002)
131. Kaberger, T.; Mansson, B.: Entropy and economic processes: physics perspectives. Ecol. Econ. **36**, 165–179 (2001)
132. Bakshi, B.R.; Gutowski, T.; Sekulic, D.: Thermodynamics and the Destruction of Resources. Cambridge University Press, Cambridge (2011)
133. Bastianoni, S.; Nielsen, S.N.; Marchettini N.; Jorgensen, S.E.: Use of thermodynamic functions for expressing some relevant aspects of sustainability. Int. J. Energy Res. **29**, 53–64 (2005)
134. Milia, D.; Sciubba, E.: Exergy-based lumped simulation of complex systems: An interactive analysis tool. Energy **31**, 100–111 (2006)
135. Odum, H.T.: Environmental Accounting. Wiley, New York (1996)
136. Sciubba, E.: Cost analysis of energy conservation systems via a novel resource-based quantifier. Energy **28**, 457 (2003)
137. Jou, D.; C-Vazquez, J.; Lebon, G.: Extended Irreversible Thermodynamics, 4th edn. Springer, London (2010)
138. Xu, M.: Thermodynamic basis of dual-phase-lagging heat conduction. J. Heat Transfer **133**, 041401-7 (2011)

139. Ottinger, H.C.: Beyond Equilibrium Thermodynamics, Wiley, New York (2005)
140. Beris, A.N.; Edwards, B.J.: The thermodynamic of Flowing Systems. Oxford University Press, New York (1994)
141. Demirel, Y.; Saxena, S.C.: Heat transfer through a low pressure gas enclosure as a thermal Insulator: design considerations. Int. J. Energy Res. **20**, 327–338 (1996)
142. Demirel, Y.; Saxena, S.C.: Heat transfer in rarefied gas at a gas-solid interface. Energy **21**, 99–103 (1996)
143. Zhdanov, V.M.; Roldugin, V.I.: Non-equilibrium thermodynamics and kinetic theory of rarefied gases. Phys.-Uspekhi. **41**, 349 (1998)
144. Sandler, S.I.: An Introduction to Applied Statistical Thermodynamics. Wiley, New York (2010)
145. Gilson, M.K.; Given, J.A.; Bush, B.L.; McCammon, J.A.: The statistical-thermodynamic basis for computation of binding affinities: a critical review. Biophysical J. **72**, 1047–1069 (1997)
146. Semenov, S.N.: Statistical thermodynamics of material transport in non-isothermal binary systems. EPL **97**, 66003 (2012)
147. Laurendeau, N.M.: Statistical Thermodynamics: Fundamentals and Applications. Cambridge University Press, Cambridge (2005)
148. Keizer, J.: Statistical Thermodynamics of Nonequilibrium Processes. Springer, Berlin (1987)
149. Ruelle, D.: Smooth dynamics and new theoretical ideas in non-equilibrium statistical mechanics. J. Stat. Phys. **95**, 393–468 (1999)
150. de Hemptinne, J.C.; Mougin, P.; Barreau, A.; Ruffine, L.; Tamouza, S.; Incheke, R.: Application to petroleum engineering of statistical thermodynamics-based equation of state. Oil Gas Sci. Technol. **61**, 363–386 (2006)
151. Giovangigli, V.; Matuszewski, L.: Supercritical Fluid Thermodynamics from Equations of State. Ecole Polytechnique, R.I. 700 (2010)
152. Müller, I.: Socio-thermodynamics—integration and segregation in a population. Contin. Mech. Thermodyn. **14**, 384–404 (2002)
153. Müller, I.: A History of Thermodynamics: The Doctrine of Energy and Entropy. Springer, London (2007)
154. Müller, I.: Extended thermodynamics: a theory of symmetric hyperbolic field equations. Appl. Math. **53**, 469–484 (2008)